Doppler-Shift Lifetime Measurements in Mg^{24}, Mg^{26}, and Si^{28}†

S. W. ROBINSON* AND R. D. BENT
Department of Physics, Indiana University, Bloomington, Indiana
(Received 11 October 1967)

The lifetimes of nuclear levels in Mg^{24}, Mg^{26}, and Si^{28} have been measured by the Doppler-shift attenuation method. Excited states were produced by inelastic scattering of 22-MeV α particles from the Indiana University cyclotron. γ-ray spectra were taken in coincidence with α-particles striking an annular detector in the backward direction. The Doppler shifts of the γ-ray peaks were attenuated by thick gold backings behind the targets, allowing the lifetimes of the levels to be calculated in terms of the attenuation and the stopping power of the gold backing. Lifetimes were measured for the 1.37-, 4.12-, and 4.23-MeV levels of Mg^{24}; the 1.81- and 2.94-MeV levels of Mg^{26}; and the 1.77-, 4.61-, and 4.97-MeV levels of Si^{28}. In addition, studies were made of the decay rates of the 5.25-, 6.01-, and 6.43-MeV levels of Mg^{24}; the triplet at 4.32–4.35 MeV in Mg^{26}; and the 6.889-MeV level in Si^{28}. The results for these three even-even s-d shell nuclei are compared with the predictions of several collective theories of nuclear structure, with shell-model calculations based on the SU_3 classification of states, and with Hartree-Fock calculations.

1. INTRODUCTION

IT has been known for some time that many $E2$ transitions in $2s$-$1d$ shell nuclei are enhanced considerably above the Weisskopf single-particle values.[1] This phenomenon is frequently attributed to collective motion of the nucleus. Further evidence for the collective nature of these nuclei is found in the fact that many of the low-lying energy levels can be arranged into overlapping rotational bands.

Previous experimental work on the nuclei Mg^{24}, Mg^{26}, and Si^{28} seems to indicate the existence of collective effects in these nuclei. The low-lying levels of Mg^{24} have been interpreted as consisting of a ground-state ($K=0$) rotational band with members at 1.368 MeV (2^+) and 4.12 MeV (4^+) and a $K=2$ rotational band built upon a γ-vibrational state at 4.23 MeV.[2,3] The 0^+ level at 6.43 MeV has been interpreted as either a one-phonon β-vibrational state or a two-phonon γ-vibrational state. Possible higher-spin members of these bands have been studied by Almqvist and Keuhner.[4]

The two lowest excited states of Mg^{26} at 1.81 and 2.94 MeV have $J^\pi=2^+$. Studies of the reaction $Al^{27}(d,He^3)Mg^{26}$ have been interpreted as evidence of a $K=0$ ground-state rotational band including the 1.81-MeV state and a $K=2$ band formed upon the 2.94-MeV level.[5,6] The triplet at 4.32–4.33–4.35 MeV is not completely understood, although its highest member has been found[7] to have $J^\pi=2^+$. γ-ray transitions from members of the triplet have been observed to the three lowest states of Mg^{26}.

In Si^{28} the evidence for rotational structure is found in the appearance of a ground-state rotational band which includes the levels at 1.77 and 4.62 MeV. A level at 8.5 MeV which decays to the 4.62-MeV $J^\pi=2^+$ state is a recent candidate for the 6^+ member of this rotational band.[8]

Measurements of electromagnetic transition rates in Mg^{24}, Mg^{26}, and Si^{28} have largely been restricted to the decay rates of the first excited states. It is of some interest for comparison with the predictions of various nuclear models to measure the γ decay rates of higher excited states, particularly those involving members of rotational bands other than the ground-state band. Since several nuclear models are frequently able to reproduce the positions and spins of the levels of a nucleus, it is important to make further transition rate measurements in order to help remove ambiguities in the interpretation of the observed structure of these nuclei. Of special interest in the present work are the analogous $2^+ \rightarrow 2^+$ transitions in the magnesium isotopes, particularly since few $M1$ transition rates have been measured in the $2s$-$1d$ shell.

The Doppler-shift attenuation method (DSAM), originated by Devons,[9] has been widely used in recent years for the measurements of short nuclear lifetimes. The method has been most successfully exploited by groups using tandem accelerators to produce heavy ion beams, and groups using the $(p,p'\gamma)$ reaction and Ge(Li) detectors. The present paper describes the study of levels in Mg^{24}, Mg^{26}, and Si^{28} excited by the 22-MeV α-particle beam of the Indiana University cyclotron.

γ-ray spectra were collected at forward and backward angles with respect to the beam direction in coincidence with pulses from inelastically scattered α particles detected in an annular solid-state detector which subtended the extreme backward angles. Doppler shifts were observed in these γ-ray spectra due to the motion

† Work supported by the National Science Foundation.
* Present address: Bartol Research Foundation, Swarthmore, Pa.

[1] H. E. Gove, Nucl. Instr. Methods **28**, 180 (1964).
[2] A. V. Cohen and J. A. Cookson, Nucl. Phys. **29**, 604 (1962).
[3] R. Batchelor, A. J. Ferguson, H. E. Gove, and A. E. Litherland, Nucl. Phys. **16**, 38 (1960).
[4] J. A. Kuehner and E. Almqvist, Bull. Am. Phys. Soc. **10**, 37 (1965).
[5] B. Cujec, Phys. Rev. **128**, 2303 (1962).
[6] F. Pellegrini and S. Wiktor, Nucl. Phys. **40**, 412 (1963).
[7] S. Hinds, H. Marchant, and R. Middleton, Nucl. Phys. **67**, 257 (1965).
[8] T. R. Canada, R. D. Bent, and J. A. Haskett, Bull. Am. Phys. Soc. **12**, 570 (1967).
[9] S. Devons, G. Manning, and D. St. P. Bunbury, Proc. Phys. Soc. (London) **A68**, 18 (1955).

of the recoil nuclei along the beam direction. The targets used in the work had thick backings of gold or magnesium, in which the recoil nuclei were stopped. The observed Doppler shifts therefore depended upon the lifetimes of the excited states involved and the times required for the recoil nuclei to stop in the backing material. For cases in which the observed shifts were less than the maximum possible shifts calculated from the kinetics of the reaction, it was possible to calculate the nuclear lifetimes from the measured attenuations of the Doppler shifts and the stopping power of the backing material.

The measurements described here include information on the lifetimes of the first seven excited states of Mg^{24}, the first two excited states of Mg^{26}, and possibly two members of the triplet at 4.35 MeV in Mg^{26}. Measurements in Si^{28} were performed on the first three excited states and the 4^+ member of the doublet at 6.88 MeV.

The results are compared in some detail with the predictions of several collective descriptions of the nucleus. These include the rotational model, the vibrational model, the Davydov-Filippov asymmetric rotator model, and the rotation-vibration interaction calculations of Faessler *et al.*[10]

Several shell-model calculations of the properties of even-even nuclei in the *s-d* shell have been made recently. The results for Mg^{24}, Mg^{26}, and Si^{28} are summarized and the few absolute transition rates which have been calculated explicitly are compared with our experimental measurements.

2. EXPERIMENTAL METHOD, APPARATUS, AND PROCEDURES

A. Method

The DSAM entails a comparison of the lifetime of an excited state in a moving nucleus with the time required for the nucleus to slow down while passing through matter. If the radiation emitted from such a nucleus is observed at two angles relative to its direction of motion, the Doppler shift seen will be reduced from the value obtained when no slowing down occurs. The reduction from the maximum shift is equal to the ratio of the average velocity of the nucleus at the instant of its decay to its initial velocity. We denote this quantity as $F(\tau)$ and it is given by

$$F(\tau)=\frac{\text{observed shift}}{\text{maximum shift}}=\frac{1}{\tau v_0}\int_0^\infty v(t)e^{-t/\tau}dt, \quad (2.1)$$

where τ is the mean lifetime of the excited state and v_0 is the initial velocity of the recoil nucleus. Therefore, in order to relate the lifetime of the excited state to the observed Doppler-shift attenuation, it is necessary to have knowledge of the rate of energy loss (dE/dx) of the recoiling nucleus so that $v(t)$ may be calculated. Lifetimes accessible to the DSAM lie in the range 10^{-11} to 10^{-14} sec.

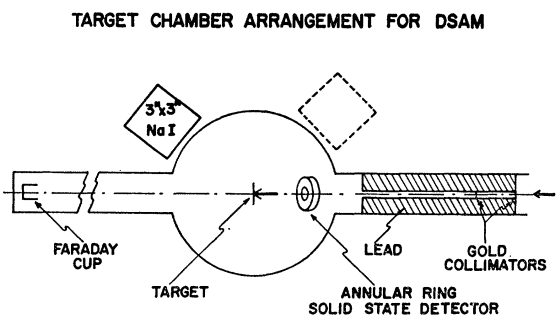

FIG. 1. Experimental arrangement.

B. Apparatus

The Indiana University Cyclotron is a 45-in.-diam fixed-frequency machine having a nominal beam energy of 21.9 MeV for α particles. The present measurements were performed in the scattering chamber shown in Fig. 1, which was enclosed in a hut of nonporous concrete with additional lead shielding along the beam pipe. The methods for performing γ-ray studies in this laboratory are described in more detail elsewhere.[11]

The scattering was performed in an 8-in.-diam chamber which had provision for the mounting of a solid-state particle detector through its rotating lid. The detector used was a silicon surface-barrier solid-state device supplied by Nuclear Diodes Inc. Its active surface was in the shape of an annulus with inner and outer diameters of 13.5 and 23 mm, respectively. This detector was mounted in the chamber so that the beam passed through its opening before striking the target and the backscattered particles were incident upon its active surface.

A 3×3-in. or 5×5-in. NaI crystal γ-ray detector could be positioned outside of the chamber at a range of angles from 40° to 140° relative to the beam direction.

Upon leaving the scattering chamber the beam passed out of the concrete hut and was collected in a tantalum Faraday cup.

Since the experiments described here were carried out over a period of almost two years, the electronic components used varied somewhat. An arrangement typical of the latter stages of the work will be described. With the exception of the Spectrastat circuit, it is essentially the standard setup used currently for particle-γ coincidence work at this laboratory.

The elements of the experimental circuitry, numbered as they appear on the block diagram (Fig. 2), are the following:

(1) The α-particle detector bias (80–100 V) was produced by an Ortec Model 210 Detector Control

[10] A. Faessler, W. Greiner, and R. K. Sheline, Nucl. Phys. **70**, 33 (1965).

[11] W. W. Eidson and R. D. Bent, Phys. Rev. **128**, 1312 (1962).

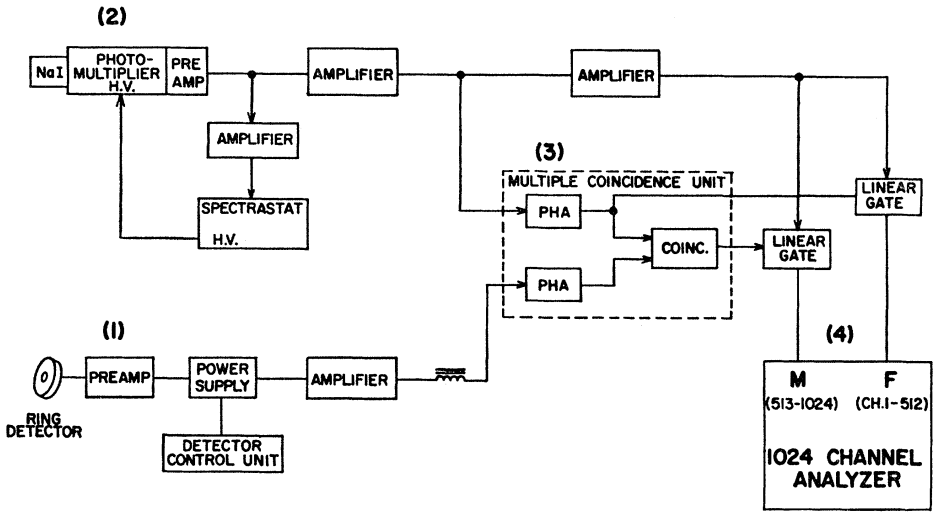

FIG. 2. Block diagram of the electronics. Numbers refer to the description in the text.

Unit, which also monitored the leakage current in the detector.

(2) The gain of the NaI crystal-photomultiplier system was stabilized by a Cosmic Radiation Laboratory Spectrastat circuit. The Spectrastat consists of a single-channel pulse-height analyzer, a counting-rate meter, and a controllable high-voltage power supply. The single-channel window was adjusted to bracket the γ-ray peak from a radioactive source (Mn^{54} or Na^{22}) placed near the NaI crystal. The circuit then adjusted the high-voltage supply to the photomultiplier to maintain the calibration peak in the center of the window. A separate amplifier was used for these pulses because it was necessary to invert their polarity so as to be compatible with the Spectrastat.

(3) The particle-γ coincidence requirement was handled by a Cosmic Model 801 Multiple Coincidence Unit. This unit consists of single-channel pulse-height analyzers (PHA) and three independent fast-slow coincidence circuits. Each PHA has a variable delay of 0–300 nsec and a fixed delay of 400 nsec. The setting chosen for the resolving time corresponded to 45 nsec (the interval between cyclotron beam pulses was 90 nsec). It was necessary to introduce an additional delay of about 200 nsec in the α-particle circuit to allow for the slower operation of the NaI photomultiplier.

(4) The coincidence output was used to trigger a linear gate (Cosmic Model 1201), through which the coincident γ's entered the Nuclear Data 150-M 1024-channel pulse-height analyzer. The analyzer was operated in the multiplex single-parameter mode (effectively as two 512-channel analyzers whose memories were broken into 256-channel blocks). Into the second analyzer input could be fed a γ-ray singles spectrum through a linear gate triggered by the output of the PHA for the γ pulses. The γ-ray singles pulse-height spectra taken in this manner were used for calibration against zero-point or gain shifts.

TABLE I. Targets and backings used for DSAM.

Nucleus	Target material	Target thickness (mg/cm²)	Backing material
Si^{28}	silicon	0.3	Au
Si^{28}	silicon	0.3	Mg
Mg^{26}	separated isotope	0.6	Au
Mg^{24}	natural magnesium	1.0	Au
Mg^{24}	natural magnesium	0.6	Au

Targets containing the nuclei to be studied were prepared on gold or magnesium backings thick enough to stop all recoil nuclei produced by inelastic α-particle scattering in the target. The thickness of the gold backing on silicon targets, for example, was 5 mg/cm². Table I lists the target materials and thicknesses and the backing materials that were used in the present experiments.

The targets were positioned perpendicular to the beam direction with the target material layer towards the incident beam.

C. Procedures

Like the electronic setup, the experimental procedures for taking data varied somewhat. The variations most commonly involved the method of using the Spectrastat stabilizing circuit and the method for calibrating against shifts in gain. The Spectrastat circuit was adjusted so that the window of its single-channel analyzer bracketed the calibration peak from Mn^{54} at 0.835 MeV (the Na^{22} 1.274-MeV peak was sometimes used). The calibration peaks were made sufficiently intense that they stood above the background level in the singles spectra by a factor of 3 to 10. The 0.835- and 0.511-MeV annihilation radiation from Na^{22} peaks in the stored singles spectrum were used to detect any shifts or drifting which may have occurred between the coincidence runs taken at the forward and backward angles.

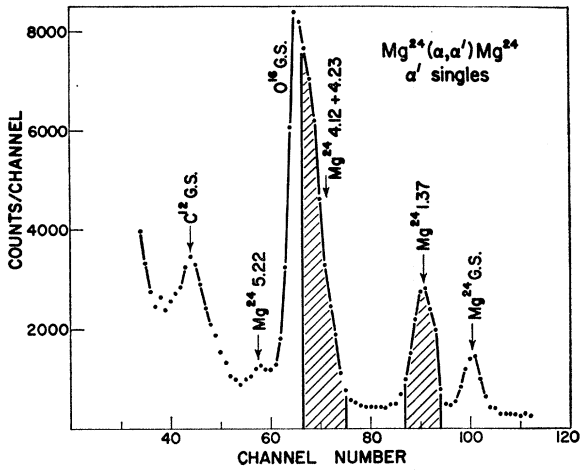

FIG. 3. Mg^{24} α-particle singles spectrum. $E_\alpha \approx 22$ MeV; $\theta_{\alpha'} \approx 166°$. The shaded areas show the window positions used for the coincidence spectra shown in Figs. 12 and 13.

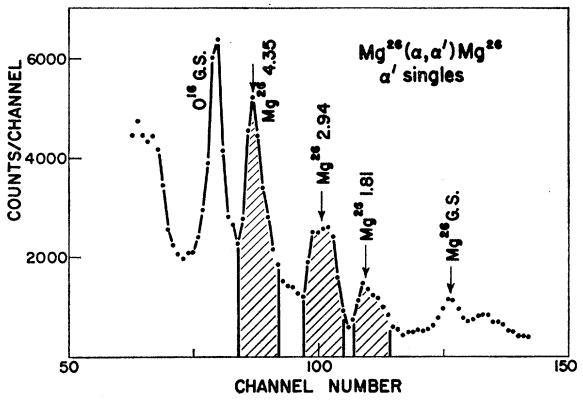

FIG. 4. Mg^{26} α-particle singles spectrum. $E_\alpha \approx 22$ MeV; $\theta_{\alpha'} \approx 166°$. The shaded areas show the window positions used for the coincidence spectra shown in Fig. 16.

The variable delays in the single-channel PHA were adjusted to obtain the maximum coincidence counting rate. The cyclotron beam pulses are about 10 nsec in duration and separated by about 90 nsec. The electronic timing was adjusted using the reaction $C^{12}(\alpha,\alpha'_{4.43}\gamma)C^{12}$ because of the high-coincidence counting rate and the well-resolved α-particle spectrum obtained from this reaction.

The resolution of peaks in the α-particle spectra was poor for two reasons: (1) In order to obtain a large coincidence counting rate, the ring detector accepted α particles scattered into a range of angles from 163.1° to 170.2°, which in the case of Mg^{24} corresponded to an energy spread of 94 keV, and (2) since moderately thick targets were selected in order to give a high counting rate, energy lost by the scattered α in the target led to an additional spread of 670 keV (for a 1.0-mg/cm² magnesium target).

The single-channel PHA on the α-particle side was adjusted to admit only one group of α particles corresponding to the state being studied. The α-particle spectra and coincidence window positions for the three nuclei studied are shown in Figs. 3, 4, and 5. Coincidences were required between these α-particle pulses and the entire γ-ray pulse-height spectrum, and the coincident γ-ray pulses were stored in a 256-channel block of the analyzer's memory.

In a second block of 256 channels a γ-ray singles pulse-height spectrum was accumulated. Since each channel in the analyzer's memory had a maximum capacity of 99 999 counts, overflow would occur in most channels if singles were collected continuously during a lengthy coincidence run. Consequently, counts were allowed to enter the singles memory only for short (2 to 5 sec) periods at regular intervals during the course of each coincidence run.

The length of the coincidence runs varied according to how much time was required to accumulate sufficient statistics in the coincidence spectra; generally 1–3-h runs with a beam intensity of 0.005 μA were required. Coincidence runs were taken alternately at the forward and backward γ-ray angles. Generally, at least two runs at each angle were made.

3. DATA ANALYSIS

A. Determination of Doppler Shifts

Peak fitting. In order to calculate the Doppler shift between a pair of γ coincidence spectra taken at different angles it was necessary to determine both the zero point of the energy calibration and the location of the centroid of the full-energy peak (photopeak) in each spectrum. The latter was accomplished by fitting the full-energy peak to the form of a Gaussian plus a background approximated by an exponential.

$$y_i = A \exp[-(\bar{x}-x_i)^2 4 \ln 2/\Delta^2] + B \exp(-Cx_i). \quad (3.1)$$

The ordinate y_i represents the number of counts in the ith channel used in the fit, x_i is the channel number of the ith channel, Δ is the full width at half-maximum,

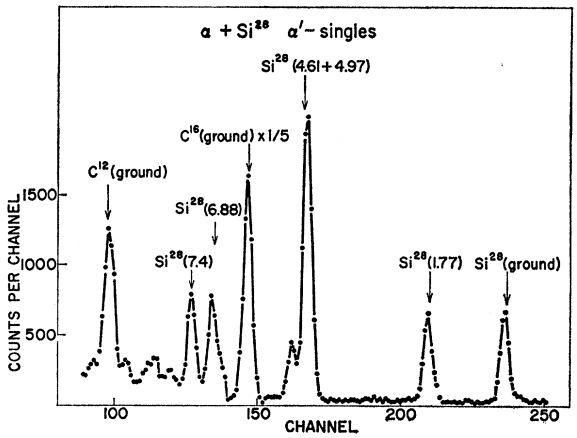

FIG. 5. Si^{28} α-particle singles spectrum. $E_\alpha \approx 22$ MeV; $\theta_{\alpha'} \approx 166°$.

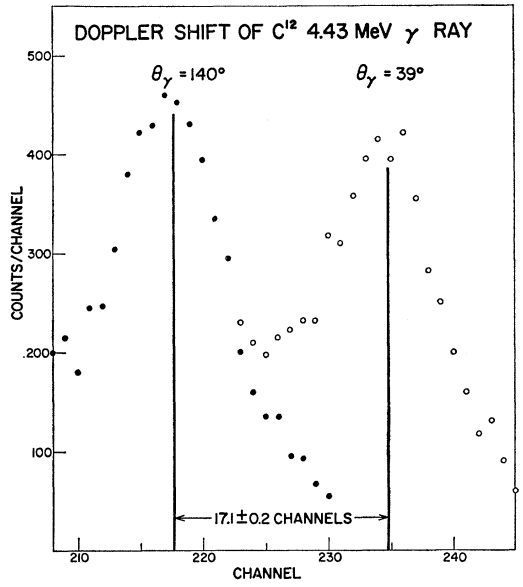

FIG. 6. γ-ray spectra at forward and backward angles from the reaction $C^{12}(\alpha,\alpha'\gamma)$ with fitted centroids.

and $\bar{x}$ is the centroid of the peak. The best fit was obtained by varying the parameters A, $\bar{x}$, Δ, B, and C in such a way as to minimize the quantity

$$\chi^2=\sum_i [y_i(\text{expt})-y_i]^2/y_i. \qquad (3.2)$$

The minimization calculations were performed on the Indiana University CDC 3600 computer using subroutine STEPIT.[12] STEPIT locates the minimum in χ^2 by varying each parameter in turn and using parabolic interpolation to obtain a new value of that parameter. The statistical errors in the determination of the centroids were also calculated by STEPIT from the shape of the χ^2 surface near the minimum. For a good fit the final value of χ^2 is expected to be about equal to the number of degrees of freedom in the fit. The number of degrees of freedom is equal to the number of channels used in the fit minus the number (five) of parameters in the fitting function. In the fitting of the coincidence peaks this criterion was in general found to be satisfied. Examples of fitted spectra are displayed in Figs. 6 and 7.

Calibration spectra. The peaks in the calibration γ-ray singles spectra were also fitted and their centroids determined. The statistical errors in this determination were very small due to the large number of counts in these peaks and it was possible to detect small shifts between the spectra. The calibration sources used were Na^{22} (0.511 and 1.27 MeV) and Mn^{54} (0.835 MeV). The 1.27-MeV peak from Na^{22} was used only in the cases where it was clearly resolved.

[12] FORTRAN code STEPIT was written by J. P. Chandler of the Indiana University Department of Physics and is distributed by the Quantum Chemistry Program Exchange, Research Computing Center, Indiana University.

Although the fits to the calibration peaks appeared visually to be very good, the χ^2 values for the best fits were frequently considerably larger than for the fits to the peaks in the coincidence spectra. This was apparently due to the fact that the shape of the full-energy peak was not exactly a Gaussian. This effect appeared only in the calibration peaks because the large number of counts in these peaks meant that this deviation was not masked by statistical fluctuations. This effect should have only a very small effect on the determination of the centroids of the peaks and, indeed, would tend to cancel out when the difference between two centroid positions was taken to determine the shift.

The small shifts observed in the calibration spectra between the forward and backward angles were found to be due to shifts in the zero point of the energy scale rather than shifts in the gain of the photomultiplier. The corrections for these shifts were of the order of 0.1 channel for peaks lying in channels 30–50.

Normalization to C^{12}. The lifetime of the 4.43-MeV first excited state of C^{12} has been measured as $\tau_m = (5.7\pm0.8)\times10^{-14}$ sec.[13] The cross section for the excitation of this level by inelastic scattering of 22-MeV α particles is large and the α-particle singles spectrum is particularly well resolved. With the α-particle window on the group from this state a γ-ray coincidence spectrum can be accumulated with very good statistics in a short time. Using a 0.1-mg/cm^2 carbon target and an average beam current of 0.005 μA, 1300 counts could be obtained in the coincidence full-energy loss peak in about 30 min. This transition was therefore chosen to calibrate our DSAM procedures. Carbon targets 0.05 to 0.15 mg/cm^2 thick with no backing material were used in these runs. Due to the very short lifetime and the absence of backing material the shift observed was expected to be very close to the maximum possible shift; that is, the shift expected from the kinematics and geometry of the runs. In all cases the observed shifts for carbon were found to be slightly less than the maximum shift calculated using the mean acceptance angle of the γ detector. The values found in various runs are given in Table II. The maximum possible shifts for other reactions were calculated for each case using the mean γ-ray angles and then were reduced using the appropriate factor from Table II. A discussion of the

TABLE II. The Doppler shifts of the C^{12} 4.43-MeV γ ray from an unbacked target.

Run No.	% of maximum shift	Detector (in.)	Range of angles
6	95.78	NaI 3×3	38° –133°
21	97.54	NaI 3×3	39° –140°
25	89.31	NaI 5×5	28½°–126°
26	88.18	NaI 5×5	36° –126°
28	92.03	NaI 3×3	36½°–137½°

[13] S. J. Skorka, J. Hertel, and T. W. Retz-Schmidt, Nucl. Data **2A**, 347 (1966).

possible errors associated with this procedure is given in Sec. 4 B.

B. Analysis of the Doppler Shifts

The analysis of the attenuated Doppler shifts measured in the manner described above depends on the calculation of the velocity of the recoiling ion $v(t)$. This requires a knowledge of the stopping power (dE/dx) for Mg^{24}, Mg^{26}, and Si^{28} ions in the gold backing as well as in the target material itself. The initial velocity of the recoil ions produced in the inelastic α-particle scattering was of the order of 10^9 cm/sec. This corresponds to 0.3 to 0.4 MeV/amu.

For ions of $Z=10$ there exists experimental stopping power data for aluminum and gold foils.[14] The aluminum data extends up to about 0.3 MeV/amu and is also available for the region above 1.0 MeV/amu.[15] In the case of gold, data exists only for energies less than 0.3 MeV/amu. In his review article Northcliffe[16] has constructed a set of smooth curves for the stopping powers of ions with $Z<10$ in carbon, aluminum, nickel, silver, and gold.

The stopping powers of magnesium and silicon were obtained from Northcliffe's aluminum curve by assuming dE/dx to be proportional to the electron density for stopping materials with atomic numbers which do not differ greatly.

In order to extrapolate the experimental stopping powers from neon to ions of higher Z the assumption was made[17] that the stopping power may be written

$$dE/dx=\langle Z^2\rangle_{\text{eff}}f(v)\,, \tag{3.3}$$

where $\langle Z^2\rangle_{\text{eff}}$ is the mean-square effective charge on the ion at velocity v. Experimental charge state studies[18] show that $\langle Z^2\rangle_{\text{eff}}$ is given approximately by

$$\langle Z^2\rangle_{\text{eff}}=Z_0^2(-0.045+57.3(V/c)Z_0^{-2/3})\,, \tag{3.4}$$

where Z_0 is the nuclear charge of the ion and V is the velocity. This relation reproduces Fig. 3 of Ref. 17. The stopping power for neon ions was then used to estimate the value for other ions by extrapolation:

$$\frac{dE_i(v)}{dx}=\frac{dE_{\text{Ne}}(v)}{dx}\frac{\langle Z_i^2\rangle_{\text{eff}}(v)}{\langle Z_{\text{Ne}}^2\rangle_{\text{eff}}(v)}. \tag{3.5}$$

For the part of the stopping power due to nuclear collisions the data of Porat and Ramavataram[14] was used. The dependence of the nuclear stopping power upon Z was approximated by $Z^{1.91}$, which is sufficient to reproduce their results. The nuclear part of the stopping power is not of great importance in the present calculations because it is appreciable only for small velocities which do not contribute appreciably to the Doppler shift.

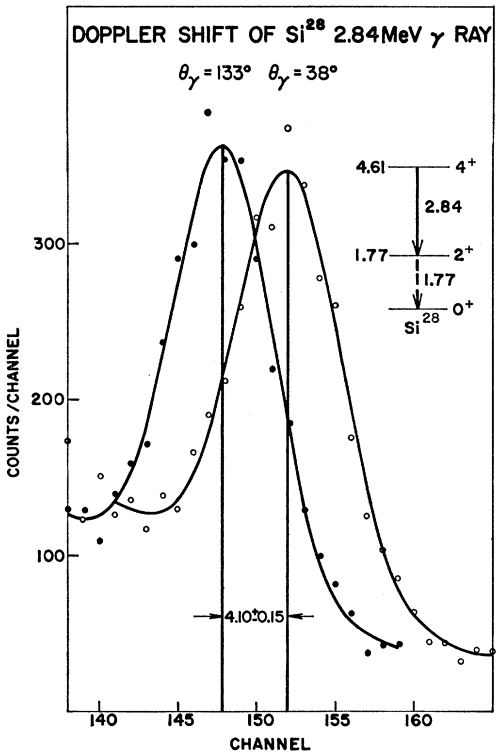

FIG. 7. γ-ray spectra at forward and backward angles from the reaction $Si^{28}(\alpha,\alpha'\gamma)$ with fitted centroids.

From the stopping power values thus obtained the velocity $v(t)$ of the recoil ions was calculated by numerical solution of the differential equation

$$dv/dt=(1/M)(dE/dx)\,. \tag{3.6}$$

The integral (2.1) was evaluated using the numerically calculated $v(t)$ in order to find the value of τ which satisfied the equality. The statistical errors in the lifetime were found by setting the right-hand side of (2.1) equal to $F\pm\Delta F$. These operations were carried out by the Indiana University CDC 3600 digital computer.

Because of the slowing which occurred in the target layer, the lifetime calculated for a given attenuation was dependent upon the position in the target at which it was assumed that the scattering occurred. Therefore, the lifetime was calculated for reactions taking place at a number of positions equally spaced across the thickness of the target layer. The lifetime values thus obtained were then averaged using Simpson's rule, and the range of the statistical errors were calculated in the same manner. It was found that only a negligible improvement was made by using more than five points in the averaging process.

[14] D. I. Porat and K. Ramavataram, Proc. Phys. Soc. (London) **78**, 1135 (1961).
[15] L. C. Northcliffe, Phys. Rev. **120**, 1744 (1960).
[16] L. C. Northcliffe, Ann. Rev. Nucl. Sci. **13**, 67 (1963).
[17] A. E. Litherland, M. L. Yates, B. M. Hinds, and D. Eccleshall, Nucl. Phys. **44**, 220 (1963).
[18] P. G. Roll and F. E. Steigert, Nucl. Phys. **17**, 54 (1960).

TABLE III. Doppler-shift attenuation measurements on Mg^{24}. The weighting factor (W) is the product of the number of runs at the forward and backward angles.

Level (MeV)	Run No.	$F(\tau)=\frac{\text{Observed shift}}{\text{Maximum shift}}$	W	Lifetime (10^{-13} sec)
1.37 (2^+)	18	0.255±0.009	6	$15.8_{-0.67}^{+0.72}$
	13	0.268±0.043	4	$12.2_{-2.1}^{+2.9}$
	Average			$14.4_{-0.88}^{+1.13}$
1.37 (2^+)	3	0.295±0.098	1	
(cascade)	17	0.175±0.063	4	
	Average	0.199±0.050		$21.5_{-5.1}^{+8.5}$
	25	0.295±0.084	4	$10.69_{-3.07}^{+5.47}$
	Average			$16.7_{-2.8}^{+5.1}$
4.12 (4^+)	3	0.977±0.068	1	
	17	0.925±0.040	4	
	Average	0.935±0.035		$0.62_{-0.33}^{+0.32}$
	25	0.961±0.057	4	$0.37_{-0.37}^{+0.47}$
	Average			$0.51_{-0.28}^{+0.33}$
4.23 (2^+)	3	1.033±0.048	1	
	17	0.679±0.148	1	
	Average	0.856±0.069		$1.36_{-0.64}^{+0.68}$
	25	0.904±0.026	4	$0.84_{-0.21}^{+0.20}$
	Average			1.01±0.25
5.25 (3^+)	24	0.91 ±0.06	4	$0.79_{-0.51}^{+0.47}$
6.01 (4^+)	22	0.89 ±0.04	2	
(4.64-MeV decay)	23	1.03 ±0.05	1	
	Average	0.94 ±0.03		$0.57_{-0.29}^{+0.28}$
6.01 (4^+)	23	0.83 ±0.13	1	$1.61_{-1.22}^{+1.39}$
(1.78–1.89-MeV decay)				
Average of both modes		0.920±0.047		$0.71_{-0.40}^{+0.37}$
6.44 (0^+)	22	0.714±0.201	2	$2.41_{-1.68}^{+2.52}$

If the excited state was produced by cascade radiation from a higher level, the shifts could be analyzed to yield the lifetime of the lower state in cases for which the lifetime of the higher state was much shorter than that of the lower state. In this case

$$F(\tau_{\text{lower}})\approx\frac{\text{Observed shift of lower state}}{\text{Observed shift of upper state}}. \quad (3.7)$$

These attenuations were analyzed in the same manner as discussed above for the Doppler shifts resulting from the decay of levels excited directly by α-particle scattering. The lifetimes obtained from the cascade transitions were used only as a check upon the values obtained from direct excitation of the level.

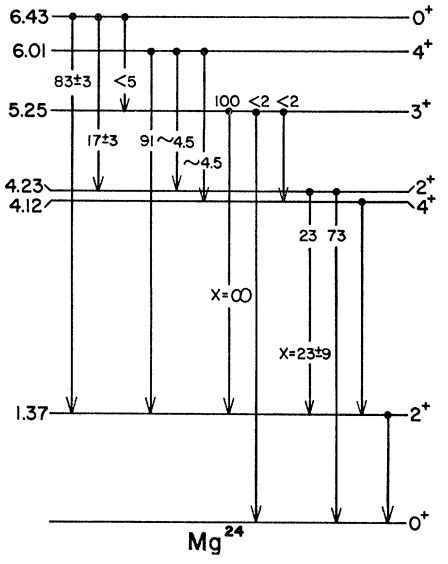

FIG. 8. Energies and decay modes of levels in Mg^{24}.

4. EXPERIMENTAL RESULTS

A. Results of the Doppler-Shift Measurements

The results which are described in this section are summarized in Tables III–IX. In Tables III–V the Doppler-shift attenuations measured in each run are tabulated along with the run number, the number of times the Doppler shift was measured (W), and the average lifetime calculated with its associated statistical error. The results from different runs are listed separately to show clearly the uncertainties associated with these measurements. Repeated measurements

agree within the combined statistical errors except for the case of the 4.23-MeV level of Mg^{24} (see the next section for a discussion of possible experimental errors). $F(\tau)$ values measured with different geometries are not averaged. The attenuations and lifetimes obtained from the cascade γ rays are also tabulated. Table VI summarizes the lifetimes measured and shows the expansions of the errors that were made to account for the uncertainty in our knowledge of the stopping powers of the target and backing materials. Tables VII–IX give the transition rate for each mode of decay. Unless indicated otherwise in the following discussion, the branching ratios and mixing ratios used are from Endt and Van der Leun.[19] These are summarized in Figs. 8–10. Tables VII–IX also contain the transition strengths in the Weisskopf units of Wilkinson,[20] with $r_0=1.25$ F.

Measurements on Mg^{24}. In the α-particle spectrum of Mg^{24} (Fig. 3) the groups from the ground state and the first excited state were clearly resolved, while the groups from the second and third excited states were masked by the strong O^{16} ground-state peak. Groups from higher levels in Mg^{24} were not well defined. The numerous earlier measurements of the lifetime of the first excited state are compared in Fig. 11. The results on the levels at 5.25, 6.01, and 6.43 MeV were obtained by varying the α-particle window position in the region below the O^{16} ground-state peak. It may be pointed out that if the α-particle scattering angle were 180° the unnatural parity level at 5.25 MeV would not be populated. The 3^+ level was excited in the present experiment because of the finite solid angle of the particle detector. Mixing ratios and branching ratios for Mg^{24} were obtained from Batchelor *et al.*[3] and Cohen and Cookson.[2] The energies of the levels are taken from Quinton and Lawrence.[21] The coincidence γ-ray spectra are shown in Figs. 12–15.

TABLE IV. Doppler-shift attenuation measurements on Mg^{26}. The weighting factor (W) is the product of the number of runs at the forward and backward angles.

Level (MeV)	Run No.	Attenuation	W	Lifetime (10^{-13} sec)
1.81 (2^+)	10	0.394±0.089	1	
	11	0.605±0.051	1	
	19	0.465±0.017	4	
	Average	0.477±0.020		$5.70_{-0.36}^{+0.39}$
1.81 (2^+) (cascade)	10	0.205±0.182	1	
	11	0.37 ±0.112	1	
	18	0.480±0.047	4	
	Average	0.417±0.046		$7.04_{-1.05}^{+1.30}$
2.94 (2^+)	10	0.793±0.075	1	
	11	0.878±0.052	1	
	18	0.774±0.042	4	
	Average	0.795±0.028		1.76±0.17
4.35 (2.54-MeV decay)	10	0.801±0.063	1	
	12	0.759±0.058	1	
	20	0.832±0.020	4	
	Average	0.815±0.019		1.60±0.09
4.35 (1.41-MeV decay)	10	0.614±0.032	1	
	20	0.978±0.107	4	
	Average	0.905±0.065		$0.86_{-0.69}^{+0.64}$

[19] P. Endt and C. Van der Leun, Nucl. Phys. **34**, 1 (1963).
[20] D. H. Wilkinson, in *Nuclear Spectroscopy*, edited by F. Ajzenberg-Selove (Academic Press Inc., New York, 1960), Part B.

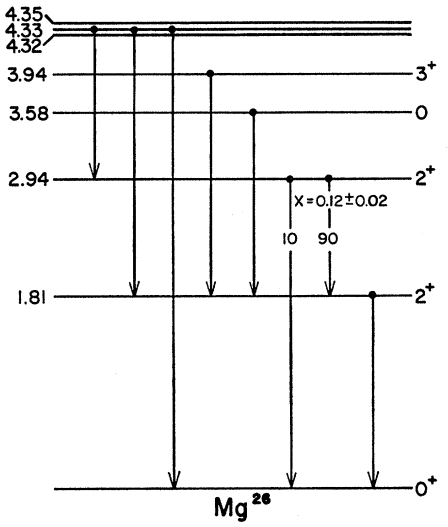

FIG. 9. Energies and decay modes of levels in Mg^{26}.

Measurements on Mg^{26}. An enriched (95%) target of Mg^{26} yielded the α-particle spectrum of Fig. 4. The particle window was placed on the resolved peaks due to the first excited state, the second excited state, and the triplet of levels at 4.32, 4.33, and 4.35 MeV. No evidence for the excitation of the levels at 3.58 and

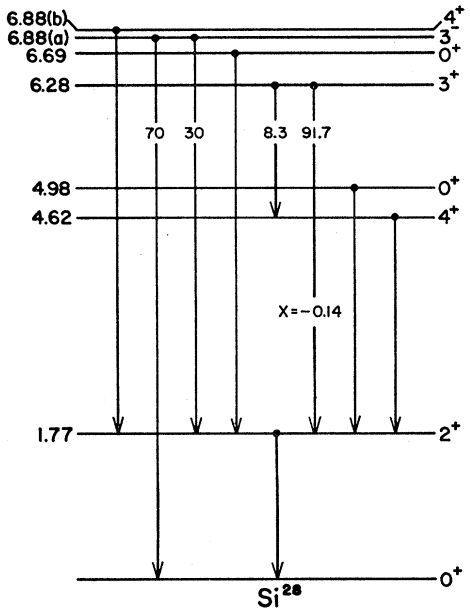

FIG. 10. Energies and decay modes of levels in Si^{28}.

[21] A. R. Quinton and G. P. Lawrence, Nucl. Phys. **37**, 244 (1962).

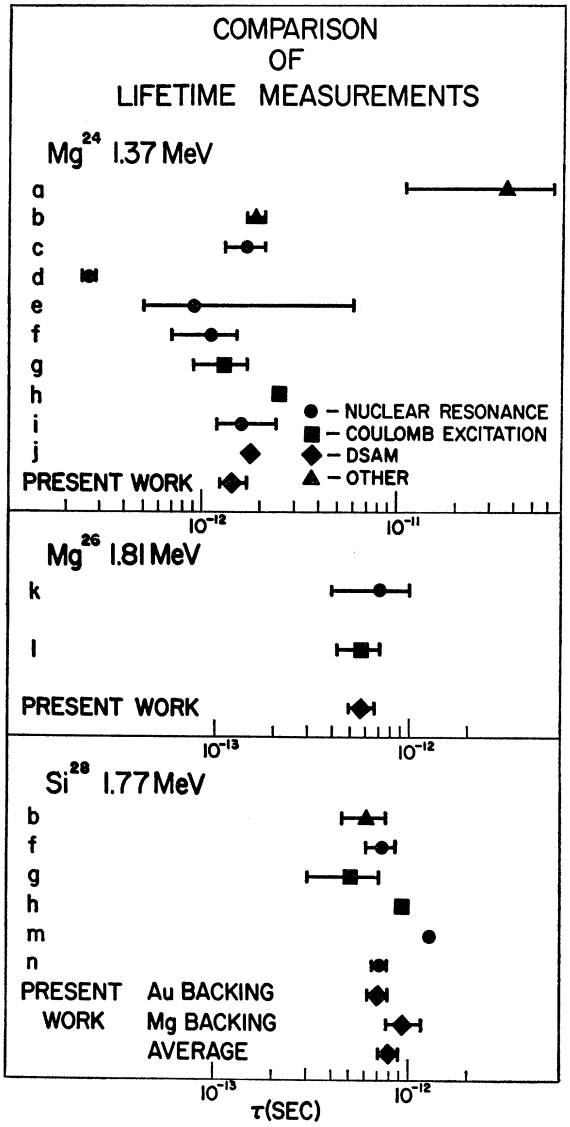

FIG. 11. Lifetime measurements of the first excited states in Mg^{24}, Mg^{26}, and Si^{28}. (a) C. F. Coleman, Phil. Mag. **46**, 1135 (1955). (b) R. H. Helm, Phys. Rev. **104**, 1466 (1956). (c) N. N. Delyagin and V. S. Shpinel, Dokl. Akad. Nauk SSSR **121**, 621 (1958) [English transl.: Soviet Phys.—Dokl. **3**, 789 (1958)]. (d) N. A. Burgov and Yu. V. Terekhov, Nucl. Phys. **10**, 941 (1959). (e) R. G. Arns, R. E. Sund, and M. L. Wiedenbeck, Phys. Rev. Letters **2**, 150 (1959). (f) S. Ofer and A. Schwartzchild, Phys. Rev. Letter **3**, 384 (1959). (g) D. S. Andreyev, A. P. Grinberg, K. I. Erokhina, and I. Kh. Lemberg, Nucl. Phys. **19**, 400 (1960). (h) H. E. Gove and C. Broude, Bull. Am. Phys. Soc. **5**, 473 (1960). (i) F. R. Metzger, C. P. Swann, and V. K. Rasmussen, Nucl. Phys. **16**, 568 (1960). (j) R. Burman and H. E. Gove (private communication, 1962). (k) V. K. Rasmussen, F. R. Metzger, and C. P. Swann, Phys. Rev. **123**, 1386 (1961). (l) D. S. Andreyev, A. P. Grinberg, K. I. Erokhina, and I. Kh. Lemberg, Isv. Akad. Nauk. SSSR, Ser. Fiz. **25**, 832 (1961). (m) E. C. Booth and K. A. Wright, Bull. Am. Phys. Soc. **6**, 37 (1961). (n) S. J. Skorka and T. W. Retz-Schmidt, Nucl. Phys. **46**, 225 (1963).

3.94 MeV was observed. The decay of the triplet was observed through γ rays of 2.54 and 1.41 MeV. A 4.35-MeV γ ray was not seen. The 1.41-MeV γ ray did not appear clearly in the spectra and the determination of its Doppler shift was less reliable than was the case for the other transitions in this nucleus. Sample γ-ray coincidence spectra are shown in Fig. 16. The lifetime which was obtained for the first excited state is compared with two earlier measurements in Fig. 11.

Measurements on Si^{28}. The lifetimes of the lowest levels in this nucleus were measured using a magnesium backing as well as a gold backing. Sample α-particle and coincidence γ-ray spectra are shown in Figs. 5, 7, 17, and 18. Lifetimes were obtained for the first excited state, the second and third excited states (which were not resolved in the α-particle spectrum), and the closely spaced doublet at 6.880–6.889 MeV [these states are referred to as 6.88(a) and 6.88(b) in the energy-level diagram]. In the first run with the latter window setting the 6.88-MeV γ ray did not appear, indicating that only the upper member of the doublet ($J^\pi=4^+$) was being excited. In the second run with this window setting the 6.88-MeV γ ray was observed in addition to the 5.11-MeV γ ray. The difference between the spectra obtained in the two runs was apparently due to a small change in the beam energy combined with a rapidly changing excitation function for the level. Unfortunately, the stabilization for the second

TABLE V. Doppler-shift attenuation measurements on Si^{28}. The weighting factor (W) is the product of the number of runs at the forward and backward angles. The target backing was gold except where otherwise indicated.

Level (MeV)	Run No.	Attenuation	W	Lifetime (10^{-13} sec)
1.77 (2^+)	1	0.162±0.028	1	
	15	0.327±0.008	9	$7.06_{-0.23}^{+0.24}$
1.77 (2^+)	1	0.229±0.118	1	
(cascade	6	0.358±0.050	1	
	7	0.324±0.021	9	
	16	0.381±0.025	4	
	14	0.362±0.061	4	
	Average	0.344±0.017		$6.59_{-0.43}^{+0.48}$
1.77 (2^+)	2	0.546±0.181	1	
Mg backing	4	0.532±0.085	1	
	21	0.576±0.091	1	
	8	0.647±0.032	6	
	Average	0.615±0.030		$9.49_{-1.13}^{+1.22}$
1.77 (2^+)	5	0.378±0.294	1	
(cascade	9	0.557±0.055	4	
Mg backing)	Average	0.521±0.046		$13.0_{-2.1}^{+2.5}$
4.61 (4^+)	1	0.663±0.049	1	
	6	1.017±0.025	1	
	7	0.881±0.009	9	
	16	0.905±0.013	4	
	28	0.977±0.037	4	
	Average	0.903±0.019		0.55±0.10
4.61 (4^+)	5	0.962±0.208	1	
(Mg backing)	9	0.963±0.028	4	
	Average	0.963±0.113		<2.25
4.97 (0^+)	28	1.061±0.049	4	<0.22
6.880 (3^-)	26	0.804±0.030	1	$1.09_{-0.17}^{+0.18}$
6.889 (4^+)	27	0.818±0.049	1	$1.01_{-0.27}^{+0.29}$

run was negated by a strong low-energy γ-ray background at the forward γ angle. To salvage the data collected, the calibration was corrected by an amount sufficient to give the same shift for the 5.11-MeV γ ray as was seen in the first run, which was properly stabilized. This procedure is of questionable nature and casts some doubt upon the result, which is already uncertain since it was obtained from only a single pair of coincidence runs. Indeed, the lifetime obtained is smaller by a factor of 20 than the result of measurements performed at Chalk River.[22] Because of these difficulties, the present result should be regarded as tentative. The branching of the 6.880-MeV state is taken from Nordhagen and Tveter[23] and the branching of the 6.26-MeV state from Cohen and Cookson.[2]

TABLE VI. Lifetime measurements with statistical errors and error adjustments for dE/dx uncertainty.

Nucleus and level (MeV)		Lifetime (10^{-13})	Statistical error	dE/dx error	Total error
	Magnesium 24				
1.37	$J=2^+$, $K=0$	14.4	$+1.13$ -0.88	$+1.24$ -1.08	$+2.37$ -1.96
4.12	$J=4^+$, $K=0$	0.51	$+0.33$ -0.28	$+0.07$ -0.02	$+0.40$ -0.30
4.23	$J=2^+$, $K=2$	1.01	$+0.25$ -0.25	$+0.10$ -0.06	$+0.35$ -0.31
5.22	$J=3^+$, $K=2$	0.79	$+0.47$ -0.51	$+0.10$ -0.02	$+0.57$ -0.53
6.00	$J=4^+$, $K=2$	0.71	$+0.37$ -0.40	$+0.09$ -0.02	$+0.46$ -0.42
6.44	$J=0^+$	2.41	$+2.52$ -1.68	$+0.39$ -0.06	$+2.91$ -1.74
	Magnesium 26				
1.81	$J=2^+$	5.70	$+0.39$ -0.36	$+0.49$ -0.43	$+0.88$ -0.79
2.94	$J=2^+$	1.76	$+0.17$ -0.17	$+0.15$ -0.13	$+0.32$ -0.30
4.35	(2.54 decay)	1.60	$+0.09$ -0.09	$+0.14$ -0.12	$+0.23$ -0.21
4.35	(1.41 decay)	0.86	$+0.64$ -0.69	$+0.14$ -0.01	$+0.78$ -0.70
	Silicon 28				
1.77	$J=2^+$ (gold)	7.06	$+0.24$ -0.23	$+0.58$ -0.55	$+0.82$ -0.78
1.77	$J=2^+$ (magnesium)	9.49	$+1.22$ -1.13	$+0.86$ -0.59	$+2.08$ -1.72
4.61	$J=4^+$	0.55	$+0.10$ -0.10	$+0.05$ -0.04	$+0.15$ -0.14
6.88	$J=4^+$	1.01	$+0.29$ -0.27	$+0.10$ -0.06	$+0.39$ -0.33
6.88	$J=3^-$	1.09	$+0.18$ -0.17	$+0.10$ -0.07	$+0.28$ -0.24

[22] A. E. Litherland, Chalk River Report, 1966 (unpublished).
[23] R. Nordhagen and A. Tveter, Nucl. Phys. **56**, 337 (1964).

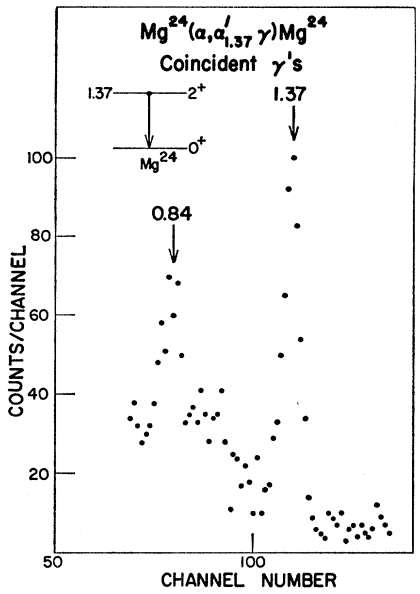

FIG. 12. Mg^{24} γ ray coincident with the 1.37-MeV α-particle group. The 0.84-MeV peak is due to accidental coincidences from the Mn^{54} calibration source.

B. Errors

Numerous uncertainties are associated with measurements of lifetimes by the Doppler-shift attenuation method. A discussion of possible sources of error and estimates of the magnitudes of these errors follows.

A major source of error in the present work was the statistical uncertainty in locating the centroid of the γ ray full-energy peak. This source of error was substantially dependent upon the cross section for excitation of the state being studied and the ratio of true to chance coincidences. If 1500 counts could be accumulated in the peak, the statistical error in the location of its centroid was of the order of 0.1 to 0.2%. This, of course, introduced a considerably larger error in the Doppler shift and hence the attenuation $F(\tau)$. In a single measurement of a Doppler shift the statistical uncertainty was of the order of 10–15% in the most favorable cases. When a number of such measurements were combined, the error affixed to the average result was the average individual error divided by the square root of the number of measurements.[24] Generally, enough measurements were made so that the statistical error was no larger than the average absolute deviation of the set of measurements from their mean value.

Another large uncertainty involved in the analysis of the shifts was in the stopping power values used. The original measurements of dE/dx have experimental errors of 5–10%.[16] Additional errors may have been

[24] F. T. Solmitz, Ann. Rev. Nucl. Sci. **14**, 375 (1964).

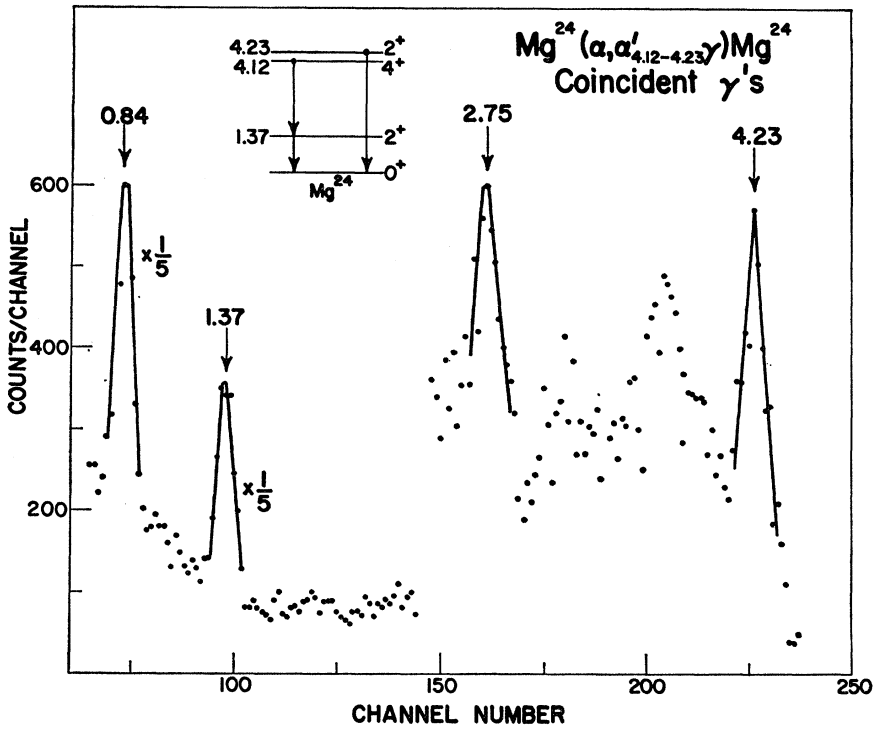

FIG. 13. Mg^{24} γ rays coincident with the 4.12- and 4.23-MeV α-particle groups.

introduced in the construction of the smoothed average curves of Northcliffe.[16] A further uncertainty was due to the extrapolation from Northcliffe's curves to the combinations of ion and stopping material used in the present work. The error introduced was greatest where extrapolation of both the ion and the stopping material was necessary, that is, for the cases where the stopping occurred mainly in the target layer, rather than in the gold backing. In Table VI the errors in the lifetimes have been enlarged to account for this uncertainty in a rather arbitrary manner; each error limit was increased by 8% of the lifetime at that limit.

The two types of error discussed thus far are the only ones which were taken into account in affixing errors to the lifetime values given in this paper. Uncertainty in the knowledge of the thickness of the target layer could have a sizable effect on the calculated lifetimes. This error is most important in cases where the target was so thick that a large part of the slowing down of the ions occurred in the target material. The effect is greatest for target materials whose stopping powers differ the most from that of the gold backing. This effect is expected to be small in the cases of short lifetimes where the decays occur mainly in the target, and of long lifetimes for which the decays occur mainly in the backing. The error in target thickness determination due to weighing was estimated to be $\pm 10\%$ for a 1.0-mg/cm^2 target. Additional errors of 5–10% could be caused by an uneven deposition in the evaporation process and the effect of heating the target frame during the evaporation, which would bake out volatile substances in the cement holding the gold foil to the frame, causing the target to appear thinner.

An uncertainty in the value of the maximum expected shift could introduce a sizable error in the lifetime obtained from the DSAM. In our experiment the uncertainty in the maximum shift arises mainly from the normalization to the measurements of the Doppler shift from the very short-lived first excited state of C^{12}. Uncertainties in the geometrical arrangement of the detectors and the target are largely removed by this normalization. On the other hand, the finite sizes of the detectors coupled with the angular distribution of the

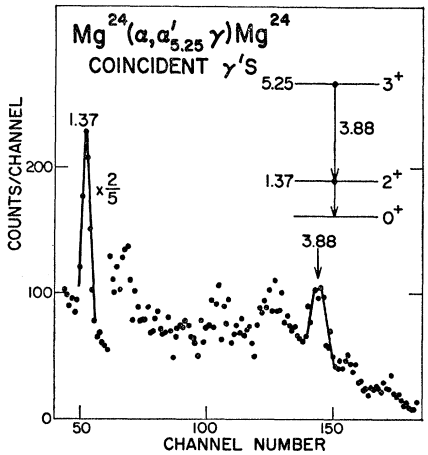

FIG. 14. Mg^{24} γ rays coincident with the 5.25-MeV α-particle group.

scattered α particles and the α-γ angular correlation introduce an uncertainty which is not the same for each nucleus. Fortunately, in our work the latter two effects are small. The angular-distribution effect would alter the effective maximum shift by only one or two tenths of a percent, while the angular correlation effect is expected to be less than 1%.

Corrections resulting from the comparison of the γ singles calibration spectra taken with each coincidence run have been discussed in a preceding section. Due to the high counting rate, the statistical uncertainty in determining the positions of the calibration peaks was very small; a few hundredths of a channel at most out of 40–50 channels. An error may have been introduced, however, by the assumption that the small shifts seen in the calibration spectra were zero-point fluctuations and not gain shifts. A gain shift not noted between the calibration peaks at 0.51 and 0.84 MeV might become appreciable at 3–4 MeV.

Another possibility of error in the calibration spectra arose from the fact that the calibration peak on which the Spectrastat stabilized was in the low-energy region and was riding upon a sloping background which was appreciable. If the intensity of this low-energy background was much larger at one of the two angles used for the coincidence spectra it would have appeared to the Spectrastat that the calibration peak had moved slightly, and the high voltage to the photomultiplier would then be adjusted to bring the peak back to the original position in the spectrum. It would then appear that there was no shift in the calibration spectra, but actually a spurious shift would have been introduced. However, a brief calculation showed that for the peak and background intensities and shapes actually encountered the shift of this type introduced by doubling the intensity of the background would be only about 0.02 channel.

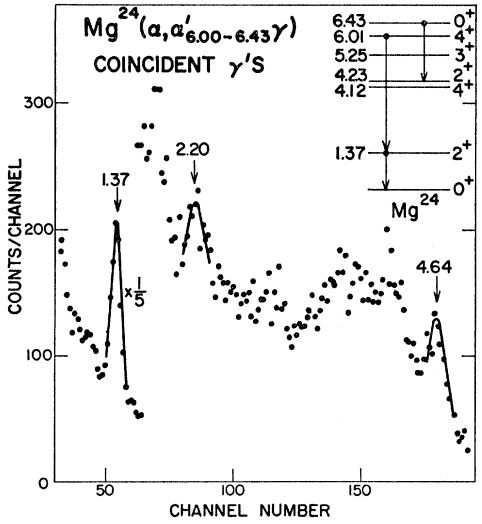

FIG. 15. Mg^{24} γ rays coincident with the 6.00- and 6.43-MeV α-particle groups.

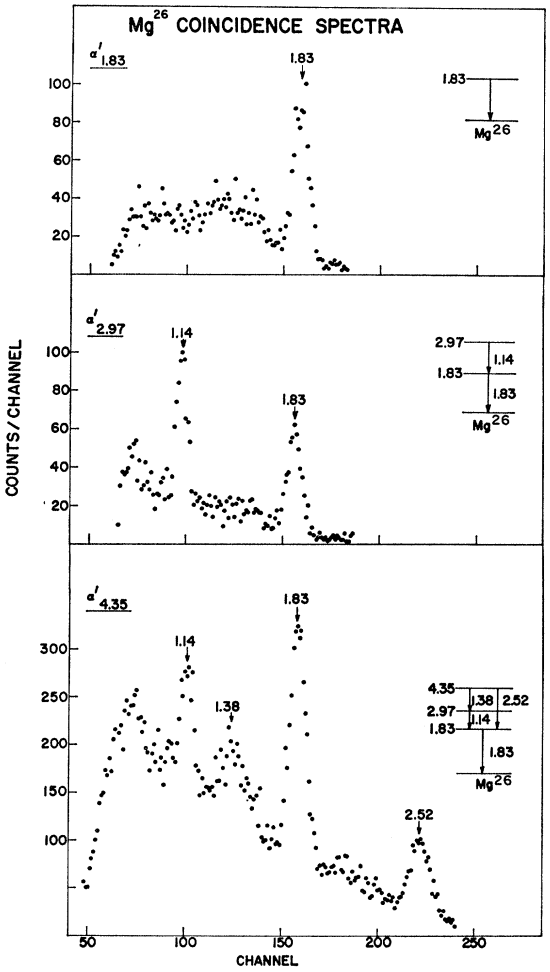

FIG. 16. Mg^{26} γ-ray coincidence spectra.

Another source of error which was considered was the effect of chance coincidences. In effect, the peak seen in the coincidence spectrum was a superposition of a peak of true coincidences and a peak consisting of chance coincidences. Thus the observed shift was an average of the actual shift of the coincidence peak and the shift of the peak in the singles spectrum weighted by the true/chance ratio. Since the shape of the chance spectrum is expected to be the same as the γ singles spectrum, this effect is most serious near strong peaks in the γ-ray singles spectra. To measure the size of this effect accidental coincidences were stored in a separate memory group of the PHA. These were obtained by varying the delay settings such that coincidences were demanded between the α-particle pulses from one beam pulse and the γ-ray pulses from the following beam pulse. Data were always taken with low beam intensity and a true/chance ratio greater than 10/1. Consequently, the error due to this effect was small.

A strong fluctuation of the cross section for excitation of the level under study over the energy range spanned by the slowing of the incident α particle in the target

TABLE VII. Measured transition rates in Mg^{24}.

Transition	Multi-polarity	Transition rate (10^{12} sec^{-1})	$\|M\|^2$
1.37 (2^+) → G.S. (0^+)	$E2$	$0.69_{-0.10}^{+0.11}$	$24.3_{-3.5}^{+3.9}$
4.12 (4^+) → 1.37 (2^+)	$E2$	20_{-9}^{+28}	$21.4_{-9.7}^{+30.0}$
4.23 (2^+) → G.S. (0^+)	$E2$	$7.6_{-2.0}^{+3.4}$	$0.95_{-0.25}^{+0.42}$
4.23 (2^+) → 1.37 (2^+)	$E2$	$2.3_{-0.6}^{+1.0}$	$2.0_{-0.5}^{+0.9}$
4.23 (2^+) → 1.37 (2^+)	$M1$	$0.0043_{-0.0026}^{+0.0125}$	$6_{-4}^{+17}\times10^{-6}$
5.25 (3^+) → 1.37 (2^+)	$E2$	13_{-5}^{+26}	$2.5_{-1.2}^{+5.0}$
6.01 (4^+) → 1.37 (2^+)	$E2$	13_{-4}^{+17}	$1.0_{-0.5}^{+1.5}$
6.01 (4^+) → 4.23 (2^+)	$E2$	>2.26	$5.0_{-2.0}^{+7.6}$
6.01 (4^+) → 4.12 (4^+)	$E2$	$1.02_{-0.55}^{+2.09}$	$3.7_{-1.5}^{+5.6}$
6.43 (0^+) → 1.37 (2^+)	$E2$	$3.4_{-2.0}^{+9.4}$	$0.17_{-0.10}^{+0.48}$
6.43 (0^+) → 4.23 (2^+)	$E2$	$0.71_{-0.44}^{+2.28}$	$2.3_{-1.4}^{+7.5}$

before scattering would cause an additional uncertainty. In calculating the lifetime we have assumed the probability of scattering to be constant across the target layer thickness, or that any small fluctuations in the excitation function average out to give a flat energy dependence.

It should be noted that the only errors quoted in the final results of this paper are the statistical errors in determining the peak shifts and the estimated errors in the dE/dx values.

5. DISCUSSION

A. Electromagnetic Transitions in the Collective Model

1. Electric Quadrupole Transitions

In the collective model the shape of the nuclear surface is given by

$$R(\theta,\varphi)=R_0[1+\sum_\mu \alpha_\mu Y_{2\mu}(\theta,\varphi)], \qquad (5.1)$$

where α_μ are the collective variables.[25]

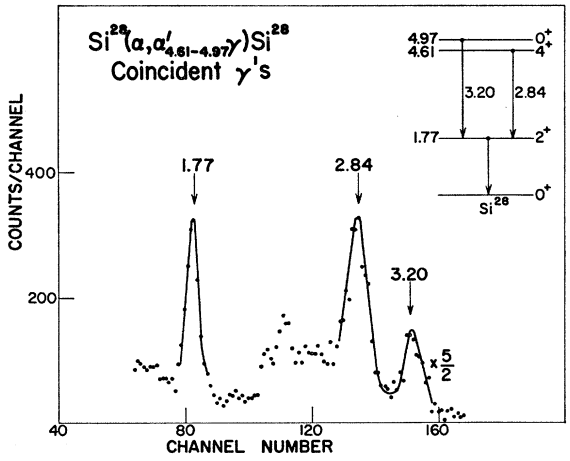

FIG. 17. Si^{28} γ rays coincident with 4.61- and 4.97-MeV α-particle groups.

[25] For example: M. A. Preston, *Physics of the Nucleus* (Addison-Wesley Publishing Co., Reading, Mass., 1962).

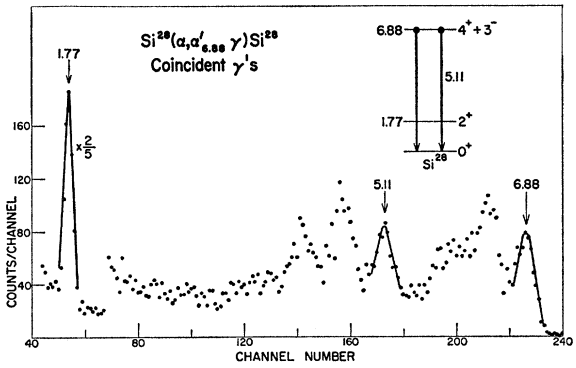

FIG. 18. Si^{28} γ rays coincident with the 6.88-MeV α-particle group.

Oscillations of the nuclear shape about a spherical equilibrium shape give rise to excited states which are (to lowest order) combinations of quadrupole vibrational phonons, each bearing $J^\pi=2^+$. $E2$ transitions involving a change of the phonon number by one show collective enhancement, while all other $E2$ transitions and all $M1$ and $E3$ transitions are forbidden to lowest order. In this model the $E2$ transition from the two-phonon level to the one-phonon level is expected to be twice as fast as the transition from the one-phonon level to the ground state.

Rotations of an axially symmetric deformed nucleus give rise to the well-known rotational energy-level spectrum. In this case the spin projection along the symmetry axis, K, is a good quantum number. Transitions among members of the ground-state ($K=0$) rotational band are related to the quadrupole moment (Q_0) of the ground state as follows:

$$B(E2;J_i\rightarrow J_f)=(C_{0^{J_f}0^2 0^{J_i}})^2(5/16\pi)e^2Q_0^2. \qquad (5.2)$$

For transitions between members of different bands the matrix element cannot be set equal to the quadrupole moment, but certain branching ratios may be calculated in terms of the Clebsch-Gordan coefficients.[26] From measured transition rates it is possible to calculate the deformation of a nucleus by use of Eq. (5.2) and the relationship

$$Q_0=3ZR_0^2(5\pi)^{-1}\beta(1+0.36\beta+0.34\beta^2+\cdots), \qquad (5.3)$$

if the nucleus is assumed to be uniformly charged.

TABLE VIII. Measured transition rates in Mg^{26}.

Transition	Multi-polarity	Transition rate (10^{12} sec^{-1})	$\|M\|^2$
1.81 (2^+) → G.S. (0^+)	$E2$	$1.8_{-0.2}^{+0.3}$	14 ± 2
2.94 (2^+) → G.S. (0^+)	$E2$	$0.57_{-0.09}^{+0.12}$	$0.39_{-0.06}^{+0.08}$
2.94 (2^+) → 1.81 (2^+)	$E2$	$0.073_{-0.011}^{+0.015}$	$6.0_{-0.9}^{+1.2}$
2.94 (2^+) → 1.81 (2^+)	$M1$	$5.1_{-0.8}^{+1.0}$	$0.11_{-0.02}^{+0.02}$
4.35 → 1.81 (2^+)	$E2$	$6.3_{-0.8}^{+1.0}$	$9.0_{-1.2}^{+1.4}$
4.35 → 2.94 (2^+)	$M1$	12_{-6}^{+51}	$0.13_{-0.07}^{+0.57}$

[26] G. Alaga, K. Alder, A. Bohr, and B. R. Mottelson, Kgl. Danske Videnskab. Selskab, Mat.-Fys. Medd. **29**, 9 (1955).

TABLE IX. Measured transition rates in Si^{28}.

Transition	Multipolarity	Transition rate (10^{12} sec^{-1})	$\|M\|^2$
$1.77(2^+) \rightarrow$ G.S.(0^+) (gold backing)	$E2$	$1.4_{-0.2}{}^{+0.2}$	
$1.77(2^+) \rightarrow$ G.S.(0^+) (average Mg and Au backing)	$E2$	$1.3_{-0.1}{}^{+0.1}$	10.3 ± 0.8
$4.61(4^+) \rightarrow 1.77(2^+)$	$E2$	$18_{-4}{}^{+6}$	$13_{-3}{}^{+4}$
$4.98(0^+) \rightarrow 1.77(2^+)$	$E2$	>50	>20
$6.88(4^+) \rightarrow 1.77(2^+)$	$E2$	$9.9_{-2.8}{}^{+4.8}$	$0.39_{-0.11}{}^{+0.19}$
$6.88(3^-) \rightarrow 1.77(2^+)$		$2.8_{-0.6}{}^{+0.8}$	
$6.88(3^-) \rightarrow$ G.S.(0^+)	$E3$	$6.4_{-1.3}{}^{+1.8}$	$320_{-65}{}^{+92}$

Davydov and co-workers[27,28] have calculated the properties of nuclei having a permanently deformed asymmetric shape. The collective variables are parametrized in such a way that for $\gamma=0°$ the model reduces to the symmetric case, while for $\gamma=30°$ the maximum asymmetry is obtained. For $\gamma=30°$ the lengths of the three axes are in the ratio 1:2:3.7. The reduced transition probabilities are all calculable in terms of the deformation parameters β and γ and are either tabulated or given in closed form in the previous references.

The rotational-vibrational model considers both rotations and vibrations about a permanently deformed axially symmetric shape. Faessler *et al.*[10] have recently discussed this model in detail. The collective variables are taken to be

$$a_0=\beta_0+a_0', \quad a_2=0+a_2', \tag{5.4}$$

where the primed quantities describe the deviation from the axially symmetric equilibrium values. Oscillations of these primed variables are analogous to vibrations of the β and γ deformation parameters. The collective Hamiltonian of Bohr and Mottelson[29] is expanded, retaining terms up to second order in a_0'/β_0 and a_2'/β_0:

$$H=T_{\text{rot}}+T_{\text{vib}}+T_{\text{vib-rot}}+V(a_0',a_2'), \tag{5.5}$$

where $V(a_0',a_2')$ is the potential energy for the vibrations. The eigenstates of

$$H_0=T_{\text{rot}}+T_{\text{vib}}+V(a_0',a_2') \tag{5.6}$$

are taken as the basis. They are given by

$$|JK;n_0n_2\rangle=\left[\frac{2J+1}{16^2(1+\delta_{K0})}\right]^{1/2}[\mathfrak{D}_{MK}{}^J+(-)^J\mathfrak{D}_{M-K}{}^J] \times\varphi_{\text{vib}}(a_0')\psi_{\text{vib}}(a_2') \tag{5.7}$$

and have energy eigenvalues

$$E_{n_0n_2}{}^{JK}=(n_0+\tfrac{1}{2})E_\beta+(2n_2+\tfrac{1}{2}K+1)E_\gamma +[J(J+1)-K^2]\tfrac{1}{2}\epsilon, \tag{5.8}$$

where $E_\beta=\hbar(C_0/B)^{1/2}$, $E_\gamma=\hbar(C_2/B)^{1/2}$, $\epsilon=\hbar^2/3B\beta_0{}^2$, and n_0 and n_2 are vibrational quantum numbers for oscillations of a_0' and a_2', respectively.

The diagonalization of $R_{\text{rot-vib}}$ on this basis was carried out by Faessler *et al.*[10] and the energies and wave functions for the various states in the ground state, β, and γ rotational bands were tabulated. The fits obtained in the present work, however, were obtained using a FORTRAN program written by Thankappan,[30] which duplicated the calculations of Faessler and in addition calculated the $E2$ transition rates.

The resulting low-lying eigenstates were found to be largely composed of the basis states $|J0;00\rangle$, $|J2;00\rangle$, and $|J0;01\rangle$. These three unperturbed bands are called the ground-state band, the γ band, and the β band, respectively. It should be noted that the rotation-vibration interaction does not mix $J=0$ levels.

The quadrupole moment operator used by Faessler *et al.* contained, in addition to the first-order term in the collective variable, a second-order term proportional to

$$(-)^\mu\sum_{\nu\sigma}C_\nu{}^2{}_\sigma{}^2{}_\mu{}^2\alpha_\nu\alpha_\sigma. \tag{5.9}$$

In their article Faessler *et al.* list explicitly the $E2$ transition matrix element in terms of the three basis states listed above.

2. *Magnetic Dipole Transitions*

The lowest-order terms of the magnetic dipole operator are given by

$$\mathfrak{M}(M1;\mu)=g^{(0)}J_\mu+g^{(1)}\sum_{\sigma\nu}C_\sigma{}^2{}_\nu{}^1{}_\mu{}^1\alpha_\sigma J_\nu. \tag{5.10}$$

It has been shown[31] that for any nucleus in which the ratio of the charge density to the mass density is a constant, i.e., the magnetic moment is parallel to the angular momentum, $g^{(0)}=Z/A$ and $g^{(1)}=0$. In this case there are no $M1$ transitions allowed by the asymmetric rotator model,[27] the rotation-vibration model,[31] or the spherical vibrator model.

In Ref. 31, Greiner considers nucleon distributions in the nucleus for which the proton and neutron distributions have different equilibrium deformations, β_p and β_n. He parametrizes the deviation from the equal-

[27] A. S. Davydov and G. F. Filippov, Nucl. Phys. **8**, 237 (1958).
[28] A. S. Davydov and V. S. Rostovsky, Nucl. Phys. **12**, 58 (1959).
[29] A. Bohr and B. R. Mottelson, Kgl. Danske Videnskab. Selskab, Mat.-Fys. Medd. **27**, 16 (1953).
[30] V. K. Thankappan (private communication).
[31] W. Greiner, Nucl. Phys. **80**, 417 (1966).

densities case by

$$f=(\beta_0-\beta_p)/\beta_0, \tag{5.11}$$

where β_0 is the deformation of the total mass distribution. Then to second order in f Greiner obtains

$$\begin{aligned} g^{(1)}&=-3(10)^{1/2}Z(1-2f)f/(2A\beta_0), \\ g^{(0)}&=Z(1-2f)(1+\tfrac{2}{3}f)/A. \end{aligned} \tag{5.12}$$

He then calculates the matrix element for $M1$ transitions on the rotation-vibration model for initial and final states given by

$$\begin{aligned} \Psi^{J_iM_i}&=A_1|J_i0;00\rangle+A_2|J_i2;00\rangle+A_3|J_i0;01\rangle, \\ \Psi^{J_fM_f}&=B_1|J_f0;00\rangle+B_2|J_f2;00\rangle+B_3|J_f0;01\rangle. \end{aligned} \tag{5.13}$$

The matrix element is given in Eq. (25) of Ref. 31 and indeed vanishes for $f=0$.

In order to estimate the value of f, Greiner uses the relation

$$\beta_p/\beta_n=[G_n/G_p]^{1/2}, \tag{5.14}$$

where G_n and G_p are the strengths of the pairing forces for neutrons and protons, respectively. For the comparisons made in our work the average of the values of Nilsson and Prior[32] and Marshalek and Rasmussen[33] is used. This gives a value $f=0.10$.

B. Comparison of Experimental Results with Collective Model Predictions

The experimentally measured transition rates will now be compared with the predictions of the various collective nuclear models.

For convenience the experimental transition rates $T(E2)$ have been converted to the reduced transition rates $B(E2)$ according to the following relation:

$$T(E2)=(4\pi/75)E^5\hbar^{-6}c^5B(E2). \tag{5.15}$$

The $B(E2)$ values thus calculated are in units of e^2f^4. The theoretical values of this quantity can be readily calculated as described in the preceding section.

The theoretical and experimental energy-level spacings and γ decay rates $[B(E2)]$ are compared for the nuclei studied in Figs. 19–21.

1. Magnesium 24

The γ decay modes of Mg^{24} have been studied previously and the data have been compared with collective nuclear models.[2,3,34] The collective nature of this nucleus is indicated by the spin sequence and spacing of its low-lying energy levels. The pattern is that of a rotational band built upon the ground state with $K=0$ and another with its band head at 4.23 MeV, having $K=2$. In the collective theory this 2^+ level is described as the one-phonon γ-vibrational state. The branching ratio of the decay of this level to the 2^+ level at 1.37 MeV and to the ground state is fairly sensitive to the assumptions of the model used to describe Mg^{24}. The large enhancement of the $E2$ decay of the first excited state has been known for some time (see Fig. 11). For our lifetime result the transition strength is 28 Weisskopf units. The assumption of a rotational nature for this transition yields an equilibrium deformation $\beta=0.51\pm0.03$. In view of these indications of collective structure in Mg^{24} it is of interest to investigate the collective model predictions regarding other electromagnetic transition rates, which are shown in Fig. 19.

First excited state (2^+, *1.368 MeV*). As noted above, this level decays by a strongly enhanced $E2$ transition. The transition rate can be fitted by the various models by adjustment of the deformation parameter β. In this work the decay rate of first excited state will be used to determine β for each model and the transition rates for the higher levels will then be calculated using the value thus obtained. Using the formula (5.3) for the quadrupole moment of a deformed drop up to third order in β we obtained $\beta=0.51\pm0.03$.

Second excited state (4^+, *4.12 MeV*). The decay of this level is also a pure $E2$ transition, leading to the first excited state. The errors associated with the present lifetime measurement encompass the predictions of all the theories considered. The pure-band rotational model predicts this transition to be 1.43 times faster than the decay of the first excited state; that is, $B(E2)=168\pm26e^2f^4$. The rotation-vibration model and the Davydov-Filippov model give similar results. In both cases the wave function of this state consists mainly of a $K=0$ ground-state rotational band component.

Third excited state (2^+, *4.23 MeV*). The decay of this level provides a more sensitive test of the theories. In the rotational model this level is interpreted as the $K=2$ γ-vibrational state. Its modes of decay are to the ground state by an $E2$ transition, and to the first excited state by a mixed $E2$-$M1$ transition ($\delta=23\pm9$, Ref. 3). The branching ratio for the $E2$ transitions is $B(E2;\ 4.23\rightarrow 1.37)/B(E2;\ 4.23\rightarrow \text{G.S.})=2.16\pm0.23$ (Refs. 2, 3, 34). The rotational model with pure K bands predicts 1.43 for this ratio; however, the predicted value is larger if the 2^+ levels contain mixtures of $K=0$ and 2 in their wave functions. It is seen from Fig. 19 that the rotation-vibration model fits to Mg^{24} give values for this branching ratio, which are too large by a factor of about 7. The asymmetric rotator model of Davydov-Filippov, when evaluated for $\gamma=22°$, which gives the best fit to the level spacing, predicts a value of 8.0 for the $B(E2;\ 2^+\rightarrow 2^+)/B(E2;\ 2^+\rightarrow 0^+)$ branching ratio, which is too large by a factor of 4. It is interesting to note that at $\gamma=12°$ a very good fit to both the branching ratio and the magnitudes of the reduced transition rates is obtained. Unfortunately, this choice of γ places the second 2^+ level at 15 MeV.

Using the mixing ratio of Batchelor *et al.* the measured $M1$ transition rate to the 1.37-MeV level is $4.3_{-2.6}{}^{+12.5}\times10^9$ sec^{-1}. The calculation of Greiner,[31] using

[32] S. G. Nilsson and O. Prior, Kgl. Danske Videnskab. Selskab, Mat.-Fys. Medd **32**, 32 (1961).
[33] E. R. Marshalek and J. O. Rasmussen, Nucl. Phys. **43**, 438 (1963).
[34] C. Broude and H. E. Gove, Ann. Phys. (N. Y.) **23**, 71 (1963).

the rotation-vibration interaction wave functions and $f=0.10$, gives an $M1$ transition rate of $T(M1)=3.2\times10^{11}$, which is too large by a factor of about 70.

Fourth excited state (3^+, *5.25 MeV*). This level is taken to be a member of the rotational band built on the γ-vibrational level at 4.23 MeV. Indeed, the analogous state in the Davydov-Filippov scheme has a wave function which is predominantly $K=2$. Cohen and Cookson[2] find that $B(E2; 5.25\rightarrow 4.12)/B(E2; 5.25\rightarrow 1.37)<12$. This is consistent with the rotational model with pure K bands which predicts 2/5 for this ratio. The rotation-vibration-model prediction for the absolute magnitude of the decay rate to the first excited state at 1.37 MeV is too small, but it is only slightly outside of the experimental error. The asymmetric rotator model prediction is in agreement with experiment for $\gamma=22°$. Alexander *et al.*[35] have recently measured the lifetime of this state to be $1.3\pm0.7\times10^{-13}$ sec.

Fifth excited state (4^+, *6.01 MeV*). The decays of the third member of the $K=2$ band to the first and second excited states (91 and 5.5–9%, respectively) are expected[2] to be largely $E2$. Thus Cohen and Cookson[2] find $B(E2; 6.01\rightarrow 4.12)/B(E2; 6.01\rightarrow 1.37)=4.9$–$8.8$, while the rotational model predicts 2.95 for pure K bands. The prediction of the rotation-vibration model for this ratio is 29, while both the rotation-vibration and Davydov-Filippov models predict absolute magnitudes for the decay to the first excited state which are smaller than experiment by a factor of 4. For the less accurately known decay branch, $B(E2;\ 6.01\rightarrow 4.12)=34.5_{-18.7}{}^{+70.8}$, there is satisfactory agreement with the rotation-vibration prediction, which is $B(E2)=33$–37.

Sixth excited state (0^+, *6.43 MeV*). This level can be interpreted either as a one-phonon β-vibrational state or as a two-phonon γ-vibrational state. The decay modes are to the 2^+ levels at 4.23 and 1.37 MeV (17 and 83%, respectively).[2] When the energy dependence is removed it is found that $B(E2; 6.43\rightarrow 4.23)/B(E2; 6.43\rightarrow 1.37)=13\pm2$. If the level is a β vibration it is expected to decay preferentially to the ground-state band, since in that case $\Delta K=0$. On the other hand, if the $n_\gamma=2$ assignment is chosen then the $|\Delta n|=1$ selection rule strongly favors decay to the γ-vibrational state at 4.23 MeV. These arguments can be put on a more quantitative footing using the rotation-vibration calculations of Faessler *et al.*[10] To test the former hypothesis ($n_\beta=1$) the parameter E_β is taken to be 6.43 MeV. Since the $J=0$ states are not mixed by the rotation-vibration interaction the energy of the β-vibrational state then coincides with the experimental value. The calculated branching ratio is then 0.15, which is to be compared with the experimental value of 13 ± 2. If the β-vibrational state is moved to higher energies, the lowest 0^+ state in the spectrum is the state $|J=0, K=0, n_2=1, n_0=0\rangle$, which is the two-phonon γ-vibrational state and falls at about 7.3 MeV. The branching ratio for decay of this state to the 4.23- and 1.37-MeV states was calculated to be about 60. Although the agreement with experiment is still not very good, the $n_\gamma=2$ assignment for the 0^+ state at 6.43 MeV is favored.

[35] T. K. Alexander, C. Broude, and A. E. Litherland, Bull. Am. Phys. Soc. **12**, 553 (1967).

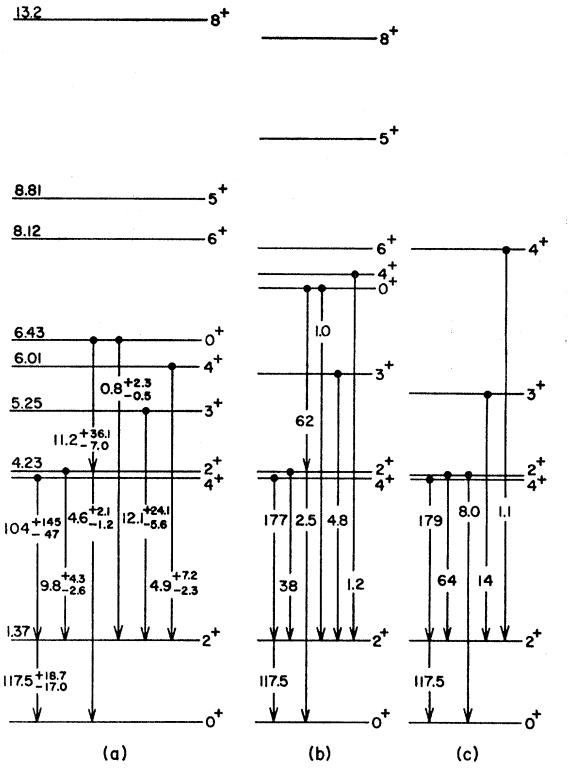

FIG. 19. (a) Experimental level structure and $B(E2)$ values for Mg^{24}. (b) Predictions of the rotation-vibration model. (c) Predictions of the Davydov model.

Summary. The present analysis shows that the collective models considered here do a satisfactory job of describing the spin sequence and spacing of the energy levels of Mg^{24}. However, the agreement between experiment and theory for the γ-decay properties of these levels is not nearly so good. In particular, the Davydov-Filippov asymmetric rotator model is unable to describe both the level spacing and the γ-decay data with the same value of the asymmetry parameter γ. Although the rotation-vibration model seems to hold the possibility of fitting the transition rates, the calculated wave functions have too much band mixing to fit the branching ratios of the 4.12- and 6.01-MeV levels.

2. *Magnesium 26*

This nucleus differs from Mg^{24} only by the addition of a pair of neutrons. However, the level spectrum of Mg^{26} differs markedly from the relatively simple rotational band structure of the lighter magnesium isotope.

Although rotational bands are not particularly obvious in this nucleus, it is still possible to fit the levels into the rotation-vibration scheme. The ground state and 1.81-MeV level can be taken as members of the $K=0$ ground-state rotational band, and the 2.94- and

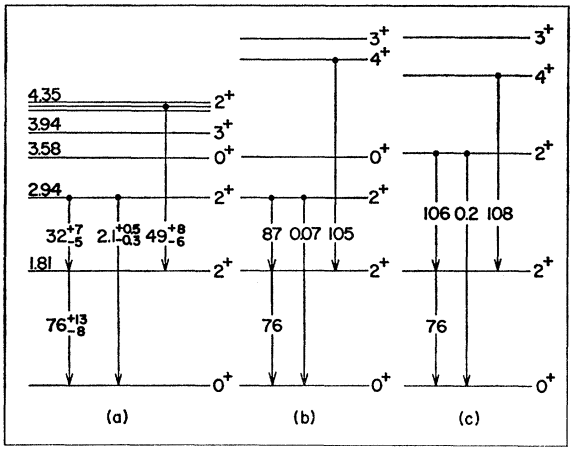

FIG. 20. (a) Experimental level structure and $B(E2)$ values for Mg^{26}. (b) Predictions of the rotation-vibration model. (c) Predictions of the Davydov model.

3.94-MeV levels as members of the $K=2$ γ-vibrational band. The $J=0$ level at 3.58 MeV may then be interpreted as the β-vibrational state. Studies of the reaction $Al^{27}(d,He^3)Mg^{26}$ have been interpreted as evidence of a $K=0$ ground-state rotational band and a $K=2$ band with its head at 2.94 MeV.[5,6]

The rotation-vibration model fit to Mg^{26} is able to reproduce the positions of the first three excited states (see Fig. 20) but gives a poor fit to the higher states.

With the asymmetric rotator model of Davydov-Filippov it is possible to obtain a low-lying second 2^+ level; however, with even the maximum asymmetry the second 2^+ level cannot be made to lie lower than twice the energy of the first excited state. Also, the 3^+ level does not fall below the 4^+ level in this model for any value of γ.

Since Mg^{26} lies near the center of the $1d_{5/2}$ shell, where nuclear deformations are believed to change from prolate to oblate shape,[36] it could have a small deformation. If this is the case, it might be expected to exhibit a vibrational spectrum. The first excited state would then be described as the one-phonon level. The degeneracy of the three two-phonon states ($0^+-2^+-4^+$) could be removed by some interaction. If the 4^+ state is assumed to be one member of the experimental triplet at 4.32–4.35 MeV, then the "center of mass" of the three assumed two-phonon levels at 2.94, 3.58, and 4.33 MeV would lie at 3.8 MeV, compared to 3.62 MeV expected from the position of the first excited state.

The γ-decay modes of the individual levels will now be discussed in terms of the rotation-vibration model, the asymmetric rotator model, and the vibrational model.

First excited state (2^+, 1.81 MeV). The $E2$ transition probability to the ground state from this level is 14 ± 2 Weisskopf units. This transition rate corresponds to a rotational transition of a uniformly charged ellipsoid with $\beta=0.41_{-0.02}{}^{+0.03}$. On the vibrational model the observed decay rate implies an oscillation about a spherical equilibrium shape with a mean effective deformation of $\beta=0.49$ (Ref. 31).

Second excited state (2^+, 2.94 MeV). This level decays to the ground state by a pure $E2$ transition and to the first excited state by a mixed $E2$-$M1$ transition with $\delta=-0.12\pm0.02$ (Ref. 34). The ratio of the reduced $E2$ transition rates $B(E2;2^+\rightarrow2^+)/B(E2;2^+\rightarrow0^+)$ is 15 ± 5. This is an even greater deviation from the prediction of pure rotational bands (1.43) than is found in Mg^{24}. As seen in Fig. 20, the rotation-vibration model predicts values which are too small for the ground-state transition and too large for the decay to the 1.81-MeV state and gives a value for the branching ratio which is much larger than experiment. For even the large asymmetry of $\gamma=20°$ the Davydov-Filippov model gives a similarly poor fit to the $E2$ decays of this level.

With the mixing ratio given above, the $M1$ decay rate of the 2.94-MeV level in Mg^{26} is found to be $5.1_{-0.8}{}^{+1.0}\times10^{12}$ sec^{-1}. It is interesting to compare this decay with the decay of the analogous state in Mg^{24}:

$$\frac{B(M1;2^{+\prime}\rightarrow2^+)_{Mg^{26}}}{B(M1;2^{+\prime}\rightarrow2^+)_{Mg^{24}}}=1.9_{-1.5}{}^{+3.9}\times10^4.$$

It is hard to reconcile this striking difference with the attempt to describe these two nuclei by the same collective nuclear models.

The theory of Greiner[31] gives for the Mg^{26} $M1$ decay rate $T(M1)=3.4\times10^{10}$ sec^{-1}.

The lifetimes of the first and second excited states of Mg^{26} have been measured recently[37] by Doppler-shift methods to be $5.3_{-1.0}{}^{+1.5}\times10^{-13}$ sec and $(2.0\pm0.8)\times10^{-13}$ sec, respectively. These results are in excellent agreement with our values.

Fifth, sixth, and seventh excited states (4.32, 4.33, and 4.35 MeV). The spins of the lower two members of this triplet (which were unresolved in the present experiment) are not known, but the spin of the state at 4.35 MeV has been determined to be 2^+. It seems likely from the systematics of $2s$-$1d$ shell nuclei that one of the lower members is a 4^+ level. Members of this triplet have been observed to decay to the ground state and the first two excited states.[19] We did not observe the ground-state transition, which is presumably due to a 2^+ member of the triplet. A 4^+ member of the ground-state rotational band would be expected to decay to the first excited state. Assuming the transition which we observed to be electric quadrupole, the value $B(E2;4.37\rightarrow1.81)=48.6_{-6.2}{}^{+7.7}e^2f^4$ is obtained. This transition rate is not inconsistent with the results for $4^+\rightarrow2^+$ transitions in Mg^{24} and Si^{28}. If the decay from the triplet to the 2^+ level at 2.94 MeV is assumed to be an $E2$ transition, a very large value of $B(E2)$ is found. On the other hand, if the $4.3\rightarrow2.94$-MeV transition is taken to be $M1$, its strength in Weisskopf units is

[36] A. Faessler (private communication, 1966).

[37] O. Häusser, T. K. Alexander, and C. Broude, Bull. Am. Phys. Soc. 12, 555 (1967).

$0.13_{-0.07}{}^{+0.57}$. This can be compared with 0.11 ± 0.02 Weisskopf units for the strength of the $2.94\rightarrow 1.81$ $M1$ transition.

These measurements suggest the following structure for the 4.32–4.35-MeV triplet in Mg^{26}: A 2^+ state decaying in part to the ground state which was not observed in this work; a 4^+ level decaying predominately to the 2^+ 1.81-MeV state; and a 2^+ or 3^+ (or even 1^+, although states of this spin and parity are uncommon in the $2s$-$1d$ shell and are not expected from the collective model approach) level which decays to the 2^+ state at 2.94 MeV by a mixed transition which is mainly $M1$.

Summary. The energy-level scheme of Mg^{26} is not fitted as readily by the collective model as that of Mg^{24}, nor are the $E2$ transition rates as adequately reproduced. The striking difference between the $M1$ transition rates in these nuclei also is not predicted.

Although the collective approach stresses points of expected similarity between the nuclei Mg^{24} and Mg^{26}, this is not the case in the shell-model description. According to the shell model, the low-lying levels of Mg^{24} are expected to have isotopic spin $T=0$, whereas the levels studied in Mg^{26} are presumed to have $T=1$. For this reason the wave functions describing states in Mg^{26} would have different symmetry from those describing states in Mg^{24}. Thus, on the basis of the shell model considerable differences might be expected in the properties of states in these nuclei. The shell-model calculations of Mg^{26} are discussed in Sec. C. In this regard, it is interesting to note that two other $T=1$ nuclei in the $2s$-$1d$ shell, Si^{30} and S^{34}, exhibit a level structure more like Mg^{26} than Mg^{24}. However, recent measurements[38] of the lifetimes of the first two excited states of Si^{30} show these decay rates to differ considerably from those for Mg^{26}. While the $M1$ strengths in the two nuclei are comparable, the $E2$ transition from the second to the first excited state is not enhanced in Si^{30}, while it shows a strength of 6 W.u. in Mg^{26}. On the other hand, the ground-state decay of the second excited state in Si^{30} is $2\frac{1}{2}$ times faster than the corresponding transition in Mg^{26}. The decays of Si^{30} have been satisfactorily explained by the treatment of this nucleus as two neutrons coupled to quadrupole oscillations of the Si^{28} core.[39]

3. *Silicon 28*

The nucleus Si^{28} is obtained by the addition of a pair of protons to Mg^{26}. As is the case for Mg^{24} and Mg^{26}, the structural differences between Mg^{26} and Si^{28} are great. The levels which comprise the supposed ground-state rotational band are present up to $J=4^+$, and recently a candidate for the 6^+ member which decays primarily to the 4^+ state at 4.62 MeV has been found[8] at about 8.5 MeV. Whereas Mg^{26} seems to exhibit a surplus of 2^+ states, in Si^{28} there is a definite lack of these levels. After the first 2^+ level at 1.77 MeV, the next known 2^+ level occurs at an excitation energy of 7.41 MeV. The absence of a lower second 2^+ level makes it impossible to attribute the 3^+ and 4^+ levels at 6.28 and 6.889 MeV to a $K=2$ rotational band. The lowest candidate for the 0^+ β-vibrational state is at 4.98 MeV, but there is another 0^+ state at 6.69 MeV which is closer to the energy of the lowest 0^+ level in Mg^{24}.

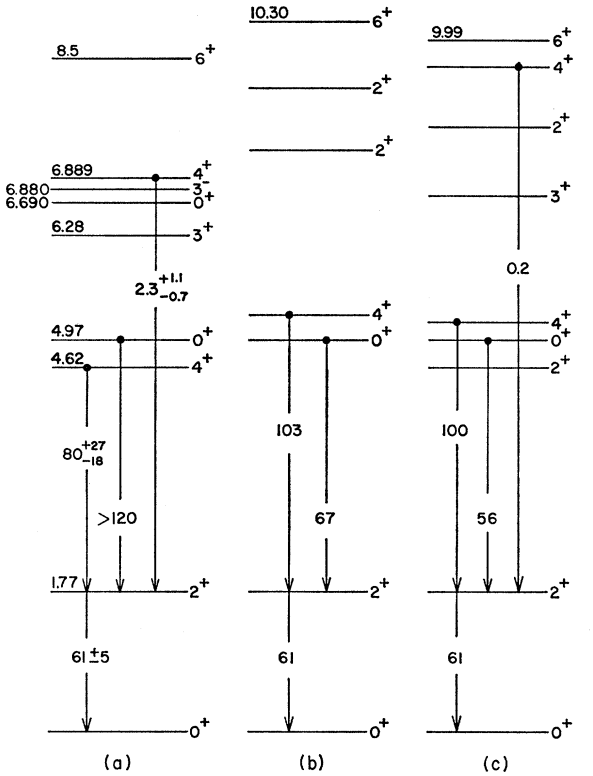

FIG. 21. (a) Experimental level structure and $B(E2)$ values for Si^{28}. (b) and (c) Predictions of the rotation-vibration model with parameters chosen to give the second 2^+ state at 7.38 and 4.62 MeV, respectively.

One member of a doublet at 6.88 MeV has been identified as a 3^- state which decays to the ground state by an enhanced $E3$ transition and to the first excited by a retarded $E1$ transition.[23,40,41]

An attempt was made to fit this nucleus with the rotation-vibration interaction model of Faessler *et al.*[10] As in the cases of Mg^{24} and Mg^{26} the parameters ϵ and E_γ of the model were selected to fit the positions of the two lowest 2^+ levels, while E_β was assigned the energy of the lowest 0^+ level. Two fits were made for different positions of the second 2^+ level (Fig. 21). In the first fit the second lowest observed 2^+ level at 7.41 MeV was used, and in the second fit the 2^+ level was assumed to be at the same energy as the experimentally observed

[38] K. P. Lieb, H. Grawe, and H. Ropke, Nucl. Phys. **A98**, 145 (1967).
[39] V. K. Thankappan and S. P. Pandya, Nucl. Phys. **39**, 394 (1962).
[40] R. Nordhagen, M. Hoffman, F. Ingebretsen, and A. Tveter, Phys. Letters **16**, 163 (1965).
[41] R. J. A. Levesque, R. W. Ollerhead, E. W. Blackmore, and J. A. Kuehner, Can. J. Phys. **44**, 1087 (1963).

4^+ level at 4.62 MeV. The latter case yielded only a slightly better fit to the higher members of the ground-state rotational band. It may be noted from Fig. 21 that the deviation of the experimental level positions from the spectrum of a rigid rotator is not great enough to give complete agreement with the rotation-vibration model calculations for the positions of the 4^+ and 6^+ members of the ground-state rotational band.

First excited state (2^+, *1.77 MeV*). The pure $E2$ decay of this state shows an enhancement of 10.3 ± 0.8. As for Mg^{24} and Mg^{26}, the deformation was calculated from the lifetime of the first 2^+ state. The value obtained in this way for Si^{28} was $\beta=0.32\pm0.01$, which is the smallest value for the three nuclei studied.

Second excited state (4^+, *4.62 MeV*). This state is presumed to be a member of the ground-state rotational band. Its $E2$ decay to the first excited state is predicted better by the rotation-vibration model than is the decay of the analogous state in Mg^{24}. In Si^{28} the reduced transition rate for the $4^+\rightarrow 2^+$ transition is greater than that for the $2^+\rightarrow 0^+$ transition. This is a prediction of all the collective models.

Third excited state (0^+, *4.95 MeV*). On the rotation-vibration model this state is taken to be the β-vibrational level. The rotation-vibration calculation predicts $B(E2; 0^+\rightarrow 2^+)=66.8e^2f^4$ while the Doppler-shift measurement places a lower limit on the transition rate of $120e^2f^4$.

Fourth excited state (3^+, *6.28 MeV*). Although the lifetime of this level was not measured it is interesting to examine its branching ratio to two members of the presumed ground-state rotational band; the 4^+ state at 4.62 MeV and the 2^+ at 1.77 MeV. The branching ratio is[2,34] $B(E2; 3^+\rightarrow 4^+)/B(E2; 3^+\rightarrow 2^+)=942$. This value is entirely inconsistent with the rotational model which predicts 0.4 for this ratio.

Seventh excited state (4^+, *6.889 MeV*). This member of the 6.880–6.889-MeV doublet[41] decays predominately to the first excited state by an $E2$ transition. It is not clear what role this level plays in the rotation-vibration model description of Si^{28}. The reduced transition probability for its decay is rather small ($2.3_{-0.7}^{+1.1}e^2f^4$), perhaps indicating that it is a member of a $K=2$ or $K=4$ band. This level is described fairly well by the calculations of Faessler *et al.* only in the case where the γ-vibrational state was taken to lie at 4.62 MeV.

Summary. We have seen that for Si^{28} there is evidence for collective motion in the existence of a fairly well-defined rotational band built upon the ground state. The $E2$ transitions within this band are adequately described by the rotation-vibration model. However, the positions and decays of the other levels do not fall easily into the collective scheme.

4. *Conclusions on the Collective Model Interpretations of Mg^{24}, Mg^{26}, and Si^{28}*

We have examined the structure of three even-even nuclei in the $2s$-$1d$ shell in terms of several collective models. In particular, detailed fits have been made to each nucleus with a rotation-vibration interaction calculation. This is a rather general collective description, which predicts both the level positions and the $E2$ and $M1$ transitions rates of specific interest to this study.

At higher masses there are known to exist extended regions throughout which collective effects dominate the nuclear structure. Thus it might be expected that if collective effects are observed in the $A=24$ region they would prevail in all three of the nuclei studied in the present work. Indeed, there are certain similarities in the structure of Mg^{24}, Mg^{26}, and Si^{28}. These are the existence of strongly enhanced $E2$ transitions, and the presence to a greater or lesser extent of rotational bands in the energy-level spectra.

More striking than the similarities, however, are the differences and trends that are observed in the structure as pairs of nucleons are added to Mg^{24}. We find that the rotation-vibration-model fit is best for Mg^{24} and becomes progressively worse for the heavier nuclei (see Sec. 5 C for a discussion of Hartree-Fock calculations, which include both particle excitations and rotational states in the description of Si^{28}). The wave functions produced by the rotation-vibration fits to the magnesium isotopes exhibit the same deviation from experimental $E2$ decay rates. The difficulty would be corrected by arbitrarily decreasing the amount of band mixing in the ground-state rotational band and increasing the amount of mixing in the $K=2$ γ-vibrational band. The opposite occurs in Si^{28}, where the rotation-vibration interaction is not great enough to reproduce the energy-level spacing of the ground-state rotational band.

In the case of the $M1$ decays, an overwhelming discrepancy of a factor of 20 000 exists between the two Mg isotopes, the transition in Mg^{26} being faster.

The apparent discrepancy in the $M1$ rates between Mg^{24} and Mg^{26} might well be a natural expectation in the shell-model description,[42,43] since in the first nucleus the states in question are all $T=0$ levels, while in the second nucleus they have isotopic spin $T=1$.

Another approach to the systematics of the even nuclei is to consider the moment of inertia of the nucleus as given by the energy-level spacing of its rotational bands. The moment of inertia can be calculated by fitting the energy levels in the ground-state band to the formula

$$E_J=(\hbar^2/2\mathcal{I})J(J+1)-BJ(J+1)^2. \qquad (5.16)$$

The moment of inertia $\mathcal{I}$ is taken in units of the moment of inertia of a rigid ellipsoid:

$$\mathcal{I}_{\text{rig}}=\tfrac{2}{5}AMR_0^2(1+0.31\beta+\cdots). \qquad (5.17)$$

In addition, the deformation of each nucleus can be estimated from the decay rate of its first excited state using Eqs. (5.2) and (5.3).

[42] G. Morpurgo, Phys. Rev. **110**, 721 (1958).
[43] E. K. Warburton, Phys. Rev. Letters **1**, 68 (1958).

For the deformed nuclei in the rare-earth region the ratio $\mathcal{I}/\mathcal{I}_{\text{rig}}$ has been plotted[25] against the deformation β. The behavior of the rare-earth nuclei is best explained by calculations on the superfluid model of nuclear matter.[44]

Figure 22 shows the region in which the rare earths and the super-fluid predictions fall. It is seen that none of the points corresponding to the $2s$-$1d$ shell nuclei shown lie in this region. However, two nuclei (Ne^{20} and Mg^{24}) which show the most rotationlike structure are close to the rare-earth nuclei in the region of large deformations. Over all, this comparison may indicate that collective rotational effects either are not of general importance in the $2s$-$1d$ shell, or are not of the same nature as those observed in heavier nuclei.

Thus we conclude that while Mg^{24} is rather well described by the collective model, there remain the details of the moment of inertia of the γ-vibrational band and the magnitude of the band mixing which are not satisfactorily reproduced. In the cases of Mg^{26} and Si^{28} we conclude that collective effects do not play such an apparent role in their structure.

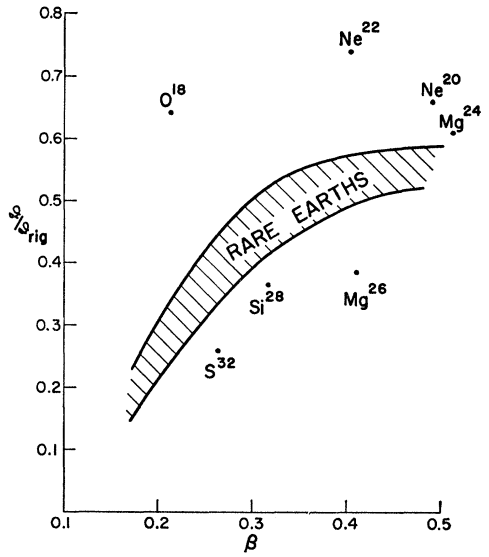

FIG. 22. The dependence of the moment of inertia upon nuclear deformation for even-even nuclei.

C. Shell-Model Calculations

There have been several recent shell-model calculations of the properties of Mg^{24}, Mg^{26}, and Si^{28}, as well as other even-even nuclei in the central part of the $s_{1/2}$-$d_{5/2}$ shell. Even though these calculations offer only a few comparisons with our transition rate measurements, they can add to our over-all understanding of the s-d shell. The papers of Stover,[45] Bouten *et al.*,[46] and Bar-Touv and Kelson[47] are treatments of extended regions of even-even nuclei in the s-d shell using the SU_3 model, intermediate coupling, and a Hartree-Fock calculation, respectively. Each approach offers an interesting over-all view of the three nuclei studied here.

General trends. From the SU_3 model we expect no $E2$ transitions between states belonging to different representations of the group. If only the partition of greatest orbital symmetry ($L=0, S=0$) is assumed to be important all $M1$ transitions are forbidden as well. Elliott and Harvey[48] point out that for Mg^{24} and Mg^{26} the representations expected to lie lowest in energy contain a $K=2$ band in addition to $K=0$, while in Si^{28} the $K=2$ band is not predicted to be present. This is in good agreement with our knowledge of these nuclei.

From work in the p shell it is expected that the α-particle nuclei will be closest to the L-S coupling limit. Indeed, in the intermediate coupling calculations of Bouten *et al.*[46] it was found that the best fits for Mg^{26} were much farther from the L-S limit than those for the α-particle nuclei Mg^{24} and Si^{28}. Stover's SU_3 calculations of the even-even nuclei in the s-d shell obtained only a poor fit to Mg^{26} (no fit was obtained for Ne^{22}).

Bar-Touv and Kelson[47] have used the Hartree-Fock method to calculate the ground states of even nuclei in the s-d shell. They have found that the lowest-lying intrinsic state in Mg^{24} is asymmetric while in Si^{28} it is symmetric. In Mg^{26} the symmetric and asymmetric states are found to lie at about the same energy. In addition Bar-Touv and Kelson observe an abrupt change in the sign of the quadrupole moment Q_0 from $+$ to $-$ between $A=26$ and 28.

Magnesium 24. In addition to the papers referred to above the structure of Mg^{24} has been the subject of two other SU_3 model calculations.[49,50] In the case of this nucleus SU_3 would appear to be particularly applicable since it has been shown that this approach is capable of producing rotational bands similar to those of an axially deformed nucleus.[51,52] In the SU_3 calculations it is assumed that the low-lying states arise from the partition of the SU_3 group possessing the maximum orbital symmetry. The various treatments differ in the number of representations of this partition included in the basis, the nature of the residual interaction, and in the inclusion of the single-particle spin-orbit force. The residual force mixes representations, while the spin-orbit interaction will mix higher partitions into the wave functions. The most detailed calculation is that of Wathne and Engeland,[50] in which all 18 representations of the partition having maximum orbital symmetry are included. The main difficulty with the spectra obtained is that the $K=2$ band begins at too low an energy. It is possible that this can be corrected by the inclusion

[44] J. J. Griffin and M. Rich, Phys. Rev. **118**, 71 (1960).
[45] J. E. Stover, Nucl. Phys. **A92**, 209 (1967).
[46] M. C. Bouten, J. P. Elliott, and J. A. Pullen, Nucl. Phys. **A97**, 113 (1967).
[47] J. Bar-Touv and I. Kelson, Phys. Rev. **138**, B1035 (1965).
[48] J. P. Elliott and M. Harvey, Proc. Roy. Soc. (London) **272**, 557 (1963).
[49] M. K. Banerjee, C. A. Levinson, and S. Meshkov, Phys. Rev. **130**, 1964 (1963).
[50] K. Wathne and T. Engeland, Nucl. Phys. **A94**, 129 (1967).
[51] J. P. Elliott, Proc. Roy. Soc. (London) **A245**, 128 (1958).
[52] J. P. Elliott, Proc. Roy. Soc. (London) **A245**, 562 (1958).

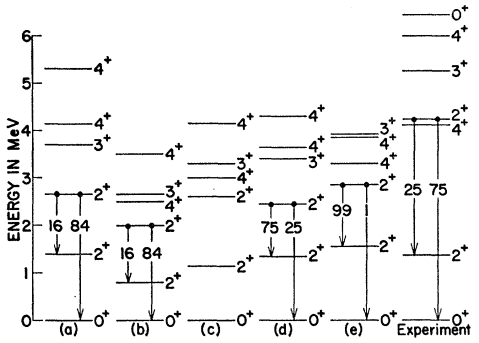

FIG. 23. SU_3 model calculations of the Mg^{24} energy levels and the branching ratio of the second excited state. (a) and (b) Elliot and Harvey (Ref. 48), Serber and Rosenfeld mixtures, respectively, no K mixing. (c) Elliot and Harvey (Ref. 48), including mixing of the three lowest representations. (d) and (e) Wathne and Engeland (Ref. 50), Serber and Rosenfeld mixtures, respectively, all representations included.

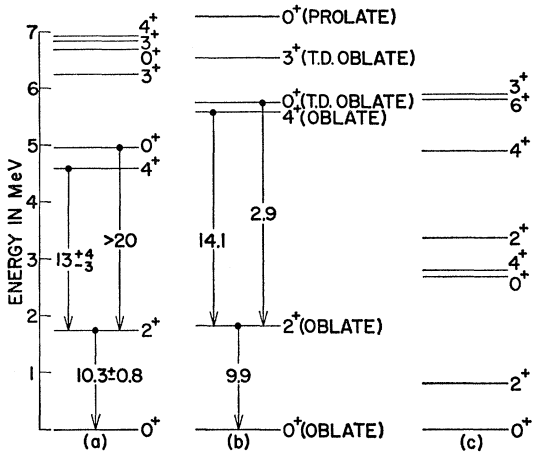

FIG. 24. Shell-model calculations of Si^{28}: (a) Experimental level scheme with $E2$ decay rates in Weisskopf units; (b) Hartree-Fock calculation of Das Gupta and Harvey (Ref. 54), with the level spacing arbitrarily increased by a factor of 2; (c) SU_3 calculation of Bernier and Harvey (Ref. 55).

of core excitations. Wathne and Engeland have also calculated the $E2$ branching ratios of a number of levels. Most interesting of these is that of the second 2^+ states. The agreement with experiment is very poor for the more realistic calculations. Typical energy-level fits and branching ratios are shown in Fig. 23.

Magnesium 26. The fits to the energy levels of this nucleus by the SU_3 model[45,46] are not particularly good (see Fig. 11 of Ref. 45 and Fig. 20 of Ref. 46). It is generally felt, however, that this model is more applicable to the α-particle nuclei, as they should be closer to the L-S coupling limit. Perhaps the weak coupling model[39] which has been successfully applied to Si^{30} could be used on this nucleus.

Silicon 28. This nucleus has been treated by the SU_3 approach,[53] the Hartree-Fock model,[54] and a particle-hole Tamm-Dancoff calculation,[53] in addition to its inclusion in the calculations for the central part of the s-d shell.[45–47] Bernier and Harvey[55] conclude that the SU_3 model fails in the case of Si^{28}. They base this conclusion on the theoretical result that the two representations lowest in energy are found to be degenerate. This degeneracy is not found experimentally, nor was it removed in the perturbation calculation which they performed. Another difficulty is found in the enhanced $E2$ decay of the second 0^+ state. In the SU_3 model this state must belong to a different representation than the first 2^+ state to which it decays and therefore the $E2$ transition is forbidden. This is interpreted as a dramatic breakdown of SU_3 symmetry, as very little mixing of configurations was found to result from the central two-body force.

Farris and Eisenberg[53] have treated Si^{28} by using the Tamm-Dancoff method with one-particle–one-hole excitations of the closed $d_{5/2}$-shell ground state, which was assumed to be spherical. Although the calculated $E2$ decay rates agree reasonably well with experiment, the energy-level spectrum is much expanded with the first excited state lying at 3.48 MeV, and the excited 0^+ states are not accounted for as they must arise from two-particle–two-hole excitations.

The Hartree-Fock (HF) calculation of Das Gupta and Harvey[54] found the lowest states of Si^{28} to be rotations of an oblate ground state and rotations of particle-hole excitations of the ground state. The third 0^+ level at 6.69 MeV can be associated with a prolate shape arising from a relative minimum in the HF calculation. The levels are given in the correct order with no extra states up to about 8 MeV; however, the spacing is compressed by about a factor of 2. In this model the enhanced decay of the second 0^+ state follows naturally since it is interpreted as a one-particle–one-hole excitation of the prolate shape to which it decays. The theoretical spectrum of Das Gupta and Harvey is shown in Fig. 24. The intermediate coupling calculation[46] finds a best fit near the L-S limit which is similar to the SU_3 calculation result of Bernier and Harvey.[55]

6. SUMMARY

It appears that the SU_3 model description of the properties of Mg^{24} is inferior to that of the collective model, particularly with respect to the $E2$ branching ratios. For Si^{28} both the SU_3 and rotation-vibration models fail and the best available fit is obtained by a HF calculation for which both particle excitations and rotational levels appear in the spectrum. As yet there are no satisfactory explanations of the structure of Mg^{26}. This nucleus appears to lie in a region where the SU_3 model is beginning to break down, and its collective features are not pronounced. It is especially difficult to explain the large $M1$ transition rate from the second 2^+ level.

[53] S. A. Farris and J. M. Eisenberg, Nucl. Phys. **88**, 241 (1966).
[54] S. Das Gupta and M. Harvey, Nucl. Phys. **A94**, 602 (1967).
[55] J. P. Bernier and M. Harvey, Nucl. Phys. **A94**, 593 (1967).